DOI: 10.4408/IJEGE.2014-01.O-02

GEOLOGICAL RISKS IN LARGE CITIES: THE LANDSLIDES TRIGGERED IN THE CITY OF ROME (ITALY) BY THE RAINFALL OF 31 JANUARY-2 FEBRUARY 2014(°)

Dario ALESSI(*), Francesca BOZZANO(*), Andrea DI LISA(*), Carlo ESPOSITO(*), Andrea FANTINI(**), Adriano LOFFREDO(*), Salvatore MARTINO(*), Francesco MELE(***), Serena MORETTO(*), Alessandra NOVIELLO(*), Alberto PRESTININZI(*), Paolo SARANDREA(**), Gabriele SCARASCIA MUGNOZZA(*), Luca SCHILIRÒ(****) & Chiara VARONE(****)

(*) Sapienza Università di Roma - Dipartimento di Scienze della Terra e Centro di Ricerca per i Rischi Gelogici (CERI) - P.le A. Moro, 5 - 00185 Roma, Italy
(**) Tecnostudi Ambiente s.r.l. - Piazza Manfredo Fanti, 30 - 00185 Roma, Italy
(***) Regione Lazio - Dipartimento Istituzionale e Territorio - Direzione Regionale Infrastrutture, Ambiente e Politiche abitative Centro Funzionale Regionale - Via Monzambano, 10 - 00185 Roma, Italy
(****) PhD student - Sapienza Università di Roma - Dipartimento di Scienze della Terra - P.le A. Moro, 5 - 00185 Roma, Italy

EXTENDED ABSTRACT

La città di Roma sorge in un contesto geologico risultante dall'azione combinata di diversi processi geologici, quali la strutturazione della Catena Appenninica, il vulcanismo della Provincia Comagmatica Romana, l'impostazione della valle alluvionale del Fiume Tevere. A tale assetto sono, di fatto, legati i diversi tipi di rischio geologico ai quali la città è esposta ovvero: sismico, vulcanico e idrogeologico, quest'ultimo comprensivo del rischio per frane, alluvioni ed inondazioni.

Il rischio sismico nella città di Roma è, invece, riconducibile a tre livelli di sismicità ciascuno dei quali è associato ad una diversa area sismo-genetica, caratterizzata da una specifica pericolosità. Questi livelli corrispondono:

- alla sismicità regionale connessa alle aree sismogenetiche dell'Appennino Centro-Meridionale (massima magnitudo attesa pari a 7);
- alla sismicità legata all'evoluzione del Distretto Vulcanico dei Colli Albani, (massima magnitudo attesa pari a 5);
- alla sismicità connessa all'area urbana (massima magnitudo attesa pari a 4).

Il rischio vulcanico della città di Roma è essenzialmente connesso alla presenza del vicino Distretto Vulcanico dei Colli Albani, oggi ritenuto in stato di "quiescenza", a cui è da aggiungere l'attività collaterale tardo-vulcanica presente su ampie zone di Roma (tra cui Ciampino) dove sono ampiamente documentate emissioni di CO_2, Metano e Radon.

Il rischio idrogeologico è, invece, principalmente connesso agli eventi di piena dei due fiumi che attraversano la città, il Tevere ed l'Aniene che già in passato sono stati causa di storiche inondazioni. Per fare riferimento al solo ultimo secolo, esemplare è stata l'esondazione del F. Tevere del dicembre 1937 che ha portato all'allagamento di ampi settori della città, tra cui la zona a monte di Ponte Milvio, l'isola Tiberina e il Lungotevere di Ripa, all'altezza di San Michele.

Per ciò che attiene i rischi idrogeologici, i numerosi rilievi collinari sui cui sorge Roma sono stati in passato interessati da numerose frane che, fatta eccezione per alcuni crolli nei depositi vulcanici, sono quasi sempre state associate a intense precipitazioni che, comunemente, sono anche responsabili di cospicue inondazioni come recentemente avvenuto nell'ottobre 2008 e 2011.

Le piogge eccezionali che hanno interessato Roma nei primi mesi del 2014 hanno riattivato alcune frane storiche, come quelle di Via A.Labriola e di Viale Tiziano, ed innescato oltre 60 nuovi fenomeni franosi. L'evento meteorologico è avvenuto tra il 31 gennaio ed il 2 febbraio 2014 ed e' stato caratterizzato da un picco di precipitazioni alle 04:00 a.m. del 31/01/2014; esso, tuttavia, ha interessato la città di Roma con intensità e durata variabili a seconda delle aree geografiche.

Un gruppo di lavoro del Centro di Ricerca per i Rischi Geologici della Sapienza (CERI) in collaborazione con il Comune di Roma (con cui è ora in essere una specifica Convenzione) e con *Roma Natura,* ha studiato l'evento meteorologico e le frane da esso innescate. A tal fine, è stato effettuato un censimento delle frane e dei danni da esse causati a strutture ed infrastrutture, una classificazione per tipologia, litologia coinvolta e parametri morfometrici dei versanti interessati. L'attività di ricerca ha permesso, inoltre, di realizzare un "Catalogo WebGIS", consultabile pubblicamente on-line dal 9 maggio 2014 sul sito del CERI (www.ceri.uniroma1.it). Le massime intensità di pioggia causate dall'evento pluviometrico sono state registrate nel settore nord-occidentale dell'area urbana, con valori di circa 105 mm di pioggia cumulata dalle 03.00 del 31 gennaio alle 03:00 del 1 febbraio. Questa intensità di pioggia è stata responsabile dell'innesco di 68 frane, perlopiù concentrate nel settore nord-occidentali di Roma (ed in particolare rilievi di Monte Mario e Monte Ciocci), dove hanno coinvolto diffusamente i depositi sabbiosi e sabbioso-limosi delle Formazioni di Monte Mario, Ponte Galeria e Valle Giulia. In base alle considerazioni qui tratte, le anomalie nella distribuzione spaziale e nella statistica per litologia degli eventi franosi censiti, rilevate rispetto agli eventi storicamente documentati, sono da mettere in relazione: i) alla distribuzione delle piogge cumulate in 6 ore, che hanno rappresentato un evento eccezionale caratterizzato da un tempo di ritorno superiore ai 50 anni; ii) al prevalente coinvolgimento del settore nord-occidentale dell'area urbana della città, dove sono presenti i rilievi collinari con maggiore dislivello; iii) al prevalente affioramento, in tale settore, di depositi clastici non vulcanici.

L'elaborato cartografico allegato al presente lavoro, riporta una sintesi iconografica delle attività di rilevamento, censimento, catalogazione ed analisi statistica condotte nel presente studio.

(°) This study was performed with the contribution of "Roma Capitale" (agreement between Roma Capitale and CERI - scientific co-ordinator Prof. A.Prestininzi)

ABSTRACT

An exceptional rainfall battered the city of Rome (Italy) from 31 January to 2 February 2014. The event had variable intensity and duration in the different parts of the city. The exceptionality of the event lies in the intensity of rainfall cumulated in 6 hours (return period > 50 years) and in its uneven distribution over the urban area. The event triggered a number of landslides of different type, which caused substantial damage. Researchers from the *Centro di Ricerca per i Rischi Geologici* (Research Centre on Prediction, Prevention and Control of Geological Risks - CERI) of the University of Rome "Sapienza" carried out field surveys and assessments immediately after the event. The team detected and inventoried 68 landslides, mostly occurring in the sandy and sandy-silty deposits of the *Monte Mario*, *Ponte Galeria* and *Valle Giulia Formations*. The complete inventory of the landslides is accessible via WebGIS on CERI's website http://www.ceri.uniroma1.it/cn/landslidesroma.jsp. The spatial distribution of the landslides evidences that 69% occurred in clastic deposits of sedimentary origin and only 6% in volcanic deposits. This finding disagrees with more general statistical data, based on the inventory of Rome's historical landslides, indicating that almost 41% of slope instabilities occur in volcanic deposits and almost 12% in sedimentary ones. In the data reported here, this apparent contradiction is justified by the fact that most the rainfall under review was concentrated in the north-western portion of Rome's urban area, whose hills accommodate outcrops of dominantly sedimentary deposits from Plio-Pleistocene marine and continental cycles.

***Key words**: Rome, exceptional rainfall in 2014, landslides, inventory, WebGIS*

INTRODUCTION

An exceptional rainfall battered the city of Rome from 31 January to 2 February 2014. The event, with peak rainfall at 4:00 a.m. of 31 Jan. 2014, had variable intensity and duration in the different parts of the city. As reported by Leone (2014) with reference to the Collegio Romano rainfall station, the intensity cumulated in the month of January 2014 can be regarded as exceptional with respect to the monthly average. The NW portions of the city recorded the highest intensity: about 105 mm of average rainfall cumulated from 3.00 a.m. of 31 Jan. to 3:00 a.m. of 1 Feb. The extremely intense rainfall triggered a number of landslides of different type in Rome's urban area, resulting into damage of variable extent. Several landslides, triggered by the intense rainfall event, were also inventoried in other areas of the Municipality, located a few kilometres away from Rome (Castiglione *et alii*, 2014). The Research Centre on Prediction, Prevention and Control of Geological Risks (CERI) of the University of Rome "Sapienza" set up a working group, which cooperated with the municipality of Rome and Roma Natura in drawing up a specific inventory. Sixty-eight landslides, mainly affecting the sandy and sandy-silty deposits of the *Monte Mario*, *Ponte Galeria* and *Valle Giulia Formations*, were identified and mapped. Most of the landslides did not cause major damage to people and property. However, 7 slope instabilities (Via della Marcigliana, Via Trionfale, Via Cavalieri di Vittorio Veneto, Via del Foro Italico, Carreggiata interna del Grande Raccordo Anulare (GRA) - inside lane of the GRA ring road, Via della Maglianella, Piazza dei Giuochi Delfici) disrupted the road network, with consequent vehicle traffic bans and inconveniences for citizens. Given the severity of the event and the number of related gravitational instabilities, technical authorities deemed it necessary to conduct a more thorough study (also as part of an agreement signed with the Municipality of Rome).

The exceptional rainfall that occurred in the winter of 2014 and the damage caused by the numerous landslides that it triggered testify, once again, Rome's susceptibility to geological hazards, which can cause substantial damage and significant levels of risk.

The city of Rome not only hosts an invaluable historical-cultural heritage, but is also the administrative hub of the Italian Republic. Its geological setting originates from a combination of processes, both geodynamic (e.g. the evolution of the Apennine chain and the volcanism of the Roman comagmatic province) and depositional (e.g. fluvial and marine sedimentation, both significantly affected by glacio-eustatic sea level changes in the Quaternary) (Faccenna *et alii*, 1995; Funiciello *et alii*, 1995; Alvarez *et alii*, 1996; Karner & Marra, 1998; Funiciello & giordano, 2008A; Funiciello & Giordano, 2008B; Parotto 2008).

The diversified geological-stratigraphic and geomorphological setting (Ascani *et alii,* 2008) of the Roman area is actually associated with different types of geological risk. The need thus arises for carrying out technical-scientific investigations to collect detailed data on critical natural events, analyse their damage scenarios, as well as their role in setting off other natural phenomena. These investigations play a crucial role in addressing and mitigating future geological risks. Indeed, they represent the groundwork for developing strategic plans aimed at preventing these risks in sensitive and critical urban areas, such as the one of the monumental "Eternal City", through emergency planning in the immediate/short term and land-use planning in the medium/long term. Mitigating these risks has become an undeferrable priority to a critical urban area like Rome, with a precious archaeological and monumental heritage and a very high population density.

In the case of Rome's urban area, the above-mentioned processes include volcanic and seismic activity, as well as floods, which should be expressed in increasing order of frequency of occurrence and damage to the city over the historically documented period.

Volcanic risk in the city of Rome is mainly related to the occurrence of the nearby Alban Hills volcanic district, whose activity began in the middle Pleistocene (Karner *et alii*, 2001B) and which now appears to be quiescent (Giordano, 2008). The current activity is concentrated in lake Albano, where strong emissions of

CO_2 (Carapezza *et alii*, 2003; Anzidei *et alii*, 2008) give evidence of confined geothermal aquifers (Giordano, 2008; Ciotoli *et alii*, 2013; Sella *et alii*, 2013). Furthermore, CO_2, methane and radon emissions are also documented in many peripheral areas of Rome (i.e. the Ciampino plain).

Conversely, Rome's seismic risk is related to 3 levels of seismicity (Molin *et alii*, 1995; DBMI, 2004; CPTI, 2004), each associated with a different seismogenetic area with a maximum expected magnitude. These levels are:

- far-field seismicity, connected with the seismogenetic areas of the central-southern Apennines, (maximum expected $6 \leq M \leq 7$), with a macroseismic intensity in Rome of up to VII-VIII MCS (Prestininzi *et alii*, 2005);
- near-field seismicity, linked to the evolution of the Alban Hills volcanic district (maximum expected $M \cong 5$);
- urban seismicity, whose epicentres are located within the city area (maximum expected $M \cong 4$).

Seismic events from these seismogenetic areas (Basili *et alii*, 2008; DISS Working Group, 2010) may generate different seismic response effects, depending on the local morphological and stratigraphic conditions of the urban area. A case in point is the recent seismic crisis of L'Aquila, associated with regional seismicity: a main shock of M_W=6.3 on 6 Apr. 2009, followed by about one hundred aftershocks, induced a felt macroseismic intensity in Rome of up to V MCS (INGV, 2009). The shaking caused damage of low, average and high degree to approximately 1,019 buildings. The damage distribution was in part controlled by the local geological setting (Bozzano *et alii*, 2011), as in the case of the felt Umbria-Marche earthquake in 1997 and by the Fucino one in 1915 (Cifelli *et alii*, 1997).

The last type of natural geological risk to which Rome is exposed is the hydrogeological one; its level of hazard is related to the occurrence of two rivers, the Tiber and Aniene, which flow into the urban area, draining part of its municipal territory and giving rise to floods after particularly intense rainfall, as happened in the past (Le Gall 1953; Frosini 1977; Luciani 1985; Bencivenga *et alii*, 1995; Remedia *et alii*, 1998) .

A case in point is the latest flood of the Tiber (December 1937), which invaded some sectors of the city, e.g. the area uphill of Ponte Milvio, the Isola Tiberina (Tiber Island) and the Lungotevere di Ripa (Ripa Tiber embankment) near San Michele. This event led technical authorities to improve flood protection and control systems by building the Corbara dam (completed in 1963).

The landslide risk is strongly linked to the aforementioned hydraulic risk. The numerous, dominantly sandy, sandy-clayey and clayey hills on which Rome rises (Heiken, 2006) historically experienced landslides of different type, intensity and recurrence. As reported by multiple historical and bibliographic sources (Colosimo, 1974; Sciotti, 1986; Prestininzi, 2000; Corazza *et alii*, 2002; Bozzano *et alii*, 2006; Amanti, 2008), these landslides (except for rock falls involving volcanic deposits) were often associated with intense precipitation; in this case, the landslides were induced by an independent natural phenomenon. Rome has never had particularly severe landslides in terms of mobilised volumes. However, there is plenty of historical records about the falls of the Rupe Tarpea (Tarpeian Rock) on the Capitoline Hill, the landslide of Viale Tiziano at the foot of the Monti Parioli hill (1972), the century-old instability of the foot of the Gianicolo hill (Via Aurelio Saffi - Via Ugo Bassi) and the more recent instabilities of Via A. Labriola, Viale Pilsudsky (Flaminio) and Via Teulada, at the foot of Monte Mario (Amanti *et alii*, 2008). It is worth noticing that most of these landslides displaced limited volumes of soil and that their intensity was low to average due, among others, to their low velocity.

The exceptional rainfall of 2014 reactivated the historical landslides of Via A. Labriola and Viale Tiziano. This paper is a technical report on the event and associated instabilities, based on field and remote surveys and assessments that inventoried the landslides and investigated the possible correlations between their type of movement and the geological and geomorphological setting of the affected areas. The field and remote surveys and assessments led, among others, to the compilation of a WebGIS inventory, which has been posted on CERI website (www.ceri.uniroma1.it) since 9 May 2014. The inventory makes the findings from the project available on line to all interested users. A workflow diagram, describing the inventory and the statistical analyses conducted as part of the project, is enclosed hereto.

ANALYSES OF THE RAINFALL EVENT

Reconstruction of the rainfall event of 31 Jan.-2 Feb. 2014

In the early hours of 31 Jan. 2014, a high-potential storm system blew through most of the Latium region (including the area of the municipality of Rome). The storm system, induced by a trough centred on the western Mediterranean, was fed by strong SE sirocco winds and by a jet stream of maritime polar air. The event caused downpours with extremely high intensity peaks (Centro Funzionale Regione Lazio, 2014).

A more detailed analysis of the event (personal communication by Andrea Luzzi Franzoni) highlights its connection with a minimum bar pressure (998 hPa) E of Majorca on 30 Jan. 2014. The event resulted from the occlusion between a cold front from the Atlantic and a warm and moist air stream from the African continent. The occlusion gave rise to a cyclonic depression, whose eye was rising and subsiding towards the gulf of Liguria (Fig. 1a). At the same time, the warm and moist air stream from Africa, no longer attracted by the cyclonic vortex, was interacting with a very moist and cold NW air stream, thereby fuelling an organised storm system, called V-shape cell, in the heart of the Tyrrhenian sea (Fig. 1b). The cell, blown northwards by southern winds, unleashed heavy and persistent rain over the coast and hinterland of Rome and, in particular, its western and south-

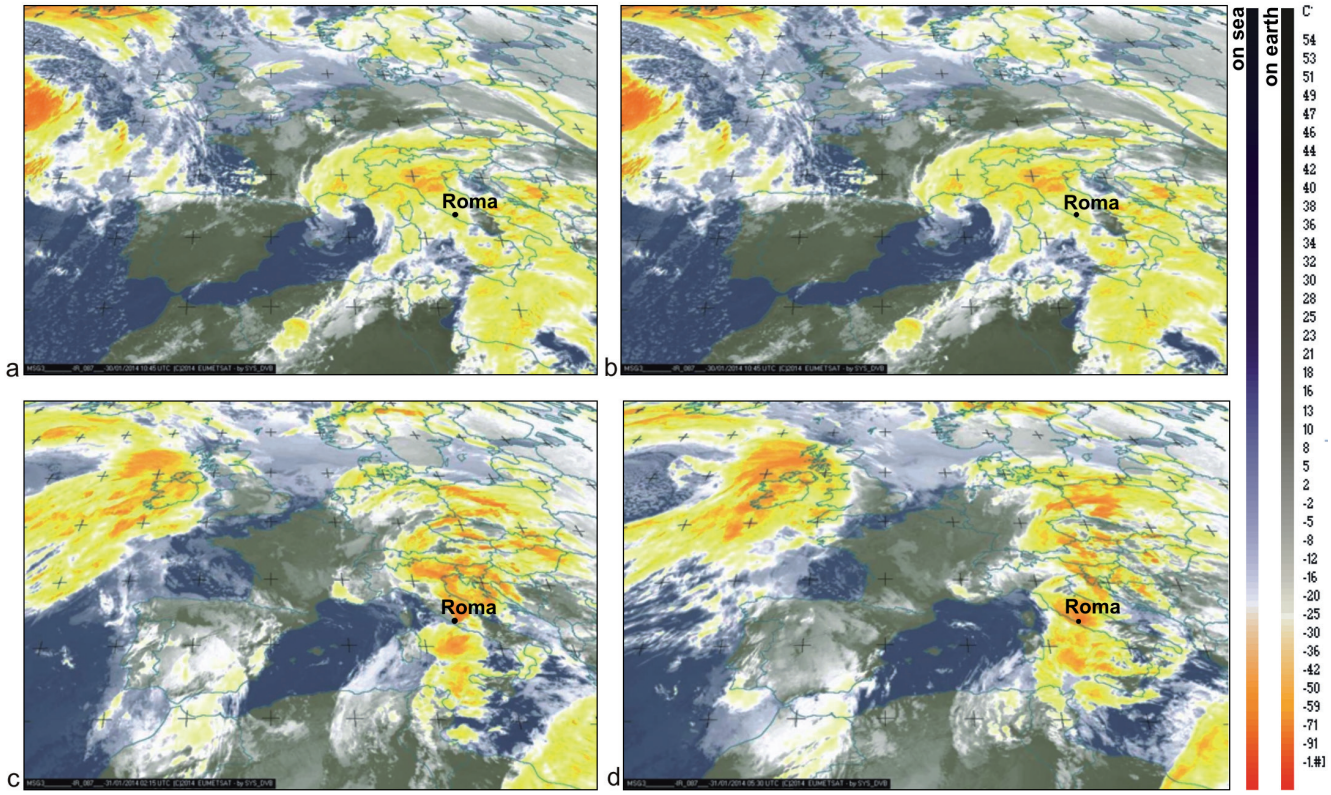

Fig. 1 - Satellite image from Meteosat MSG3, IR 8.7 channel (infrared), with filter-enhanced colour; filter applied to estimate cloud top temperature (in °C) and height. Lower temperatures are indicative of a higher cloud top, as in the case of congested cumulonimbuses with severe storms. In particular, temperature distribution can give an improved understanding of the "physics" of the phenomenon (e.g. the probability of formation of ice at high altitude). The number-colour scale only applies to clouds: a) 10:45 a.m. UTC, 30 Jan. 2014; b) 9:00 p.m. UTC, 30 Jan. 2014; c) 2:15 a.m. UTC, 31 Jan. 2014; d) 5:30 a.m. UTC, 31 Jan. 2014 - Source: EUMETSAT

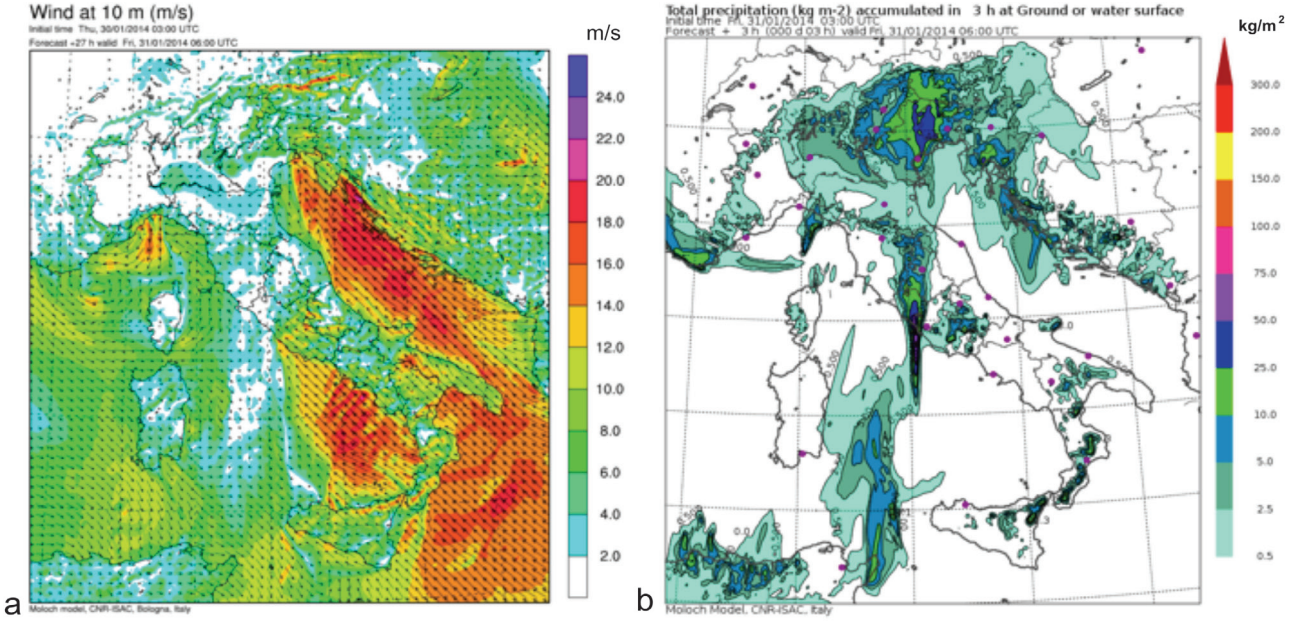

Fig. 2 - Weather forecast at 6:00 a.m. UTC, 31 Jan 2014: a) wind map; b) precipitation map. (Archivio Previsioni Meteorologiche CNR-ISAC)

western metropolitan area. The cell was then deviated towards NE by southern winds (Figs. 1c-1d; 2a), battering the coast of Rome (Fig. 2b) and its hinterland and, in particular, its western and SW metropolitan area with intense and persistent rain.

Based on the data recorded by 30 rainfall stations operating in Rome upon the event (Fig. 3a and Plate I, section 2), the rainfall cumulated from 31 Jan. to 3 Feb. 2014 was equal to about 148 mm on average, but much above 200 mm at some stations (e.g. about 252 and 245 mm at the Ottavia and Roma Monte Mario stations, respectively).

However, in this time interval, two main sub-events may be distinguished. The first (and most severe in terms of amount of rainfall) started in the early hours of 31 Jan. and ended after about 24 hours, with an average cumulated rainfall of about 105 mm and hourly intensity peaks exceeding 40 mm in some cases (e.g. 46 mm at the Roma Monte Mario station). The second sub-event, of shorter duration and with less intensity peaks, took place in the afternoon of 2 Feb., from about 1:00 to 6:00 p.m., with a total average cumulated rainfall of approximately 25 mm and maximum hourly peaks slightly above 10 mm (e.g. 11.2 mm at the Ottavia station).

Use was made of the Thiessen polygon method in a GIS environment to estimate the areal distribution of the rainfall associated with the above-mentioned two events. Rainfall, especially on 31 Jan., was clearly concentrated in north-western Rome, in terms of both maximum hourly peak (at 4:00 a.m., Fig. 3b) and cumulated values for the entire event (Fig. 3c). The areal rainfall associated with the event of 2 Feb. (Fig. 3d) shows the same pattern, albeit less clearly.

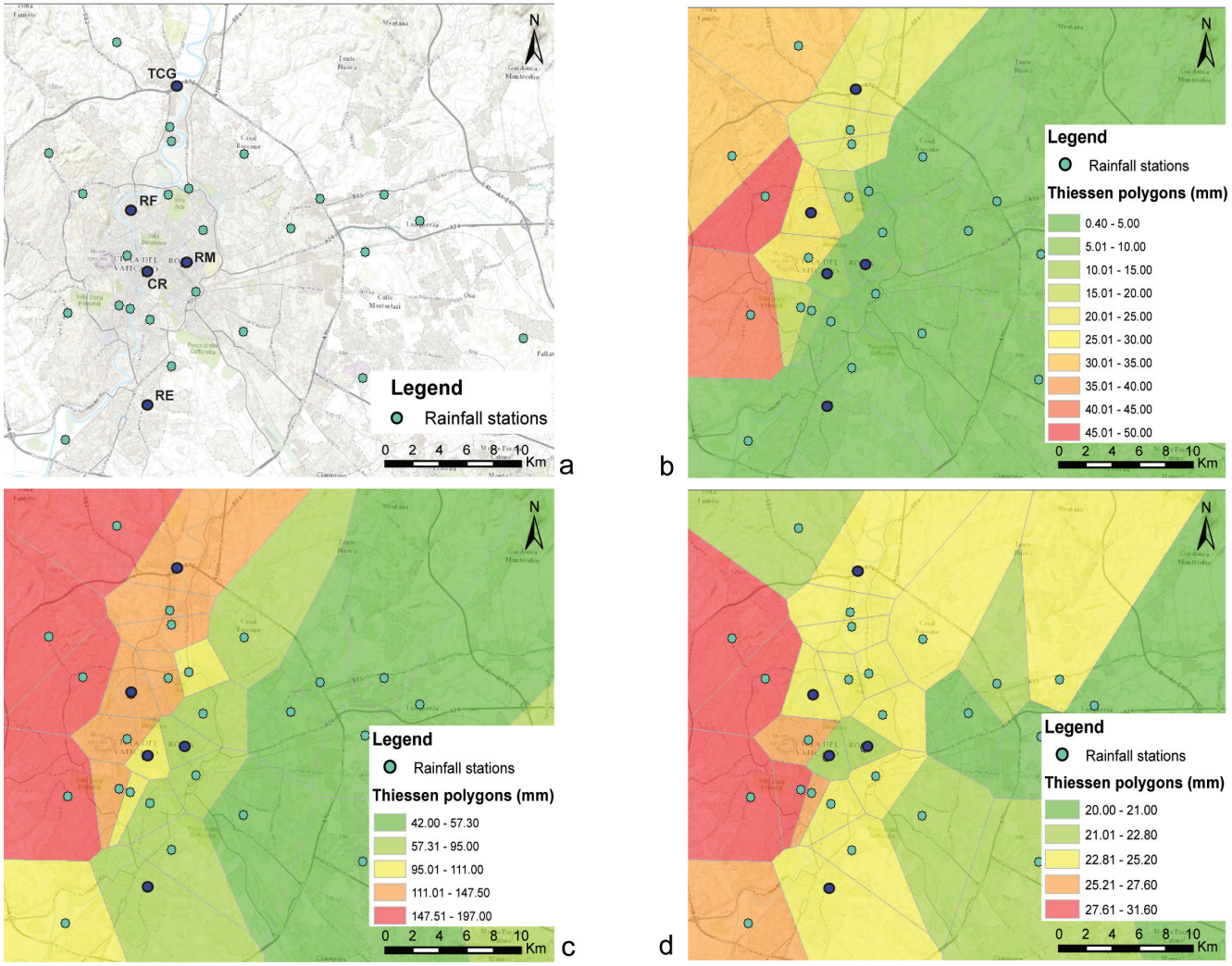

Fig. 3 - a) location of the 30 rainfall stations operating in the area of the municipality of Rome during the event of the winter of 2014; b) areal rainfall cumulated from 3:00 to 4:00 a.m. UTC, 31 Jan 2014; c) areal rainfall cumulated during the event of 31 Jan. 2014 (from 3:00 a.m. UTC of 31 Jan. 2014 to 3:00 a.m. UTC of 1 Feb. 2014); d) areal rainfall cumulated during the event of 2 Feb. 2014 (from 1:00 p.m. UTC of 2 Feb. 2014 to 6:00 p.m. UTC of 2 Feb. 2014)

	Acqua Acetosa	Aniene a Lunghezza	Aniene a Ponte Salario	Aurelio	Capannacce	Casilino	Cassiodoro	Collegio Romano	Eleniano
Recording time (years)	19	21	22	19	10	21	19	62	18
Time interval of maximum continuity of the data (years)	1993-2011	2001-2011	1993-2011	2002-2011	1993-2011	1964-2013	1994-2011	1964-2013	1994-2011
	Eur	Flaminio	Fosso di Pratolungo	Monte Mario	Ostiense	Ottavia	Regillo	Roma Bufalotta	Roma Est
Recording time (years)	18	8	29	19	18	19	11	18	19
Time interval of maximum continuity of the data (years)	1999-2011	2004-2011	1997-2012	1993-2011	1999-2011	1993-2011	1994-2004	2007-2013	1993-2011
	Roma EUR	Roma Flaminio	Roma Macao	Roma Monte Mario	Roma Monte Mario (Villa Mille Rose)	Roma Nord	Roma Sud	Rosolino Pilo	Salone
Recording time (years)	52	42	62	6	35	19	19	14	22
Time interval of maximum continuity of the data (years)	1964-1994	1974-1987	1988-2013	2007-2013	1964-1999	1994-2011	1993-2011	2007-2011	1950-1959
	Tevere a Castel Giubileo	Tevere a Fidene	Tevere a Porta Portese	Tor Marancia	Tor Vergata	Via Marchi			
Recording time (years)	46	7	17	8	19	15			
Time interval of maximum continuity of the data (years)	1953-1973	2006-2013	2002-2013	2007-2013	2002-2013	2002-2011			

Tab. 1 - Time series continuity distribution for the daily rainfall data recorded by the stations located in the area of the municipality of Rome

Assessment of the event return period

Estimating the return period for an event similar to the one described here requires analysing the time series of daily rainfall in the study area, in order to check, first of all, the continuity of the data. Tab. 1 displays the recording time interval of each station that was and/or is operational in the area of the municipality of Rome.

Unfortunately, out of the 33 stations identified, very few had statistically significant datasets. Many stations had been in place for relatively few years (since the early 1990s) and had recorded data in a discontinuous way. Therefore, to build the statistical hydrological model of the study area, use was made of data from the following 5 stations: Collegio Romano, Roma Eur, Roma Macao, Roma Flaminio and Tevere Castel Giubileo. Even if the latter two stations had more discontinuous records than the other three, they were included in the analysis, taking into account the long timespan investigated.

Therefore, consideration was given to the daily rainfall data collected since 1952 (Collegio Romano, Roma Eur and Tevere Castel Giubileo stations), 1953 (Roma Macao station) and 1957 (Roma Flaminio station). The probability model relied on the Generalized Extreme Value (GEV) distribution introduced by Jenkinson (1955), whose probability function is:

$$F_{X_{(x)}} = exp\left\{-\left[1-\frac{k(x-u)}{\alpha}\right]^{1/k}\right\}; k \neq 0$$

where μ and α are the location and scale parameters, respectively, whereas k (shape parameter) expresses the type of distribution. This distribution is a generalised version of the more known Gumbel distribution (whose function coincides with the GEV one, when k is equal to 0), largely used in the study of extreme events.

The variables of "rainfall cumulated" in 2, 5, 10, 30, 60, 90, 120 and 180 days were computed from daily rainfall data. The maximum values of each variable were extracted, year by year, from the datasets so generated and the parameters k, α and μ of the GEV function were determined from the above values, by applying the Probability Weighted Moments (PWM) method introduced by Greenwood *et alii* (1979) and subsequently modified by Hosking *et alii* (1984). Finally, the inversion of the probability function yielded the values of cumulated rainfall x for each of the variables (2, 5, 10..… 180 days) and for 6 different return periods (2, 4, 10, 20, 50 and 100 years). Then, these values were interpolated with a view to building the rainfall probability curves.

The comparison of the different curves obtained for the 5 stations (Fig. 4) reveals that, return period remaining equal, the curves of Tevere Castel Giubileo and Roma Flaminio are those with the highest rainfall values. This finding emphasises that, in the past, the two stations (the most representative of the sector most severely hit by the event of 2014, i.e. the one of the NW quadrant of the city) had recorded more intense and severe rainfall than the other three.

Tab. 2 exhibits the estimated return periods, based on the above curves, for rainfall cumulated until 30 Jan. (the day prior to the peak event) and until 31 Jan., respectively. The values infer that rainfall cumulated until 30 Jan., at all the stations, is far from exceptional (estimated return periods of 1-2 years); thus, rainfall prior to the critical event practically lies within the standard range, in contrast with rainfall cumulated until 31 Jan.

In this case, while rainfall recorded at Roma Eur and Roma Macao continues to be unexceptional, rainfall cumulated in 2 days (30 and 31 Jan.) at Roma Flaminio and Tevere Castel Giubileo has a return period of 15 and 20 years, respectively. Conversely, the Collegio Romano station, with an estimated return period of 9 years, ranks in an intermediate position. This means that the event under review was not only strongly localised in space, but also particularly severe in that specific sector of the city. This finding is also substantiated by what has been previously pointed out, i.e. the highest return periods were obtained for the stations with the highest rainfall probability curves.

Considering that only the event of 31 Jan. had a seemingly exceptional nature, the same statistical analysis was carried out on the historical data of maximum intensity rainfall (measured in 1, 3, 6, 12 and 24 hours) recorded by the same stations. The curves so built (Fig. 5) have a different pattern with respect to daily ones.

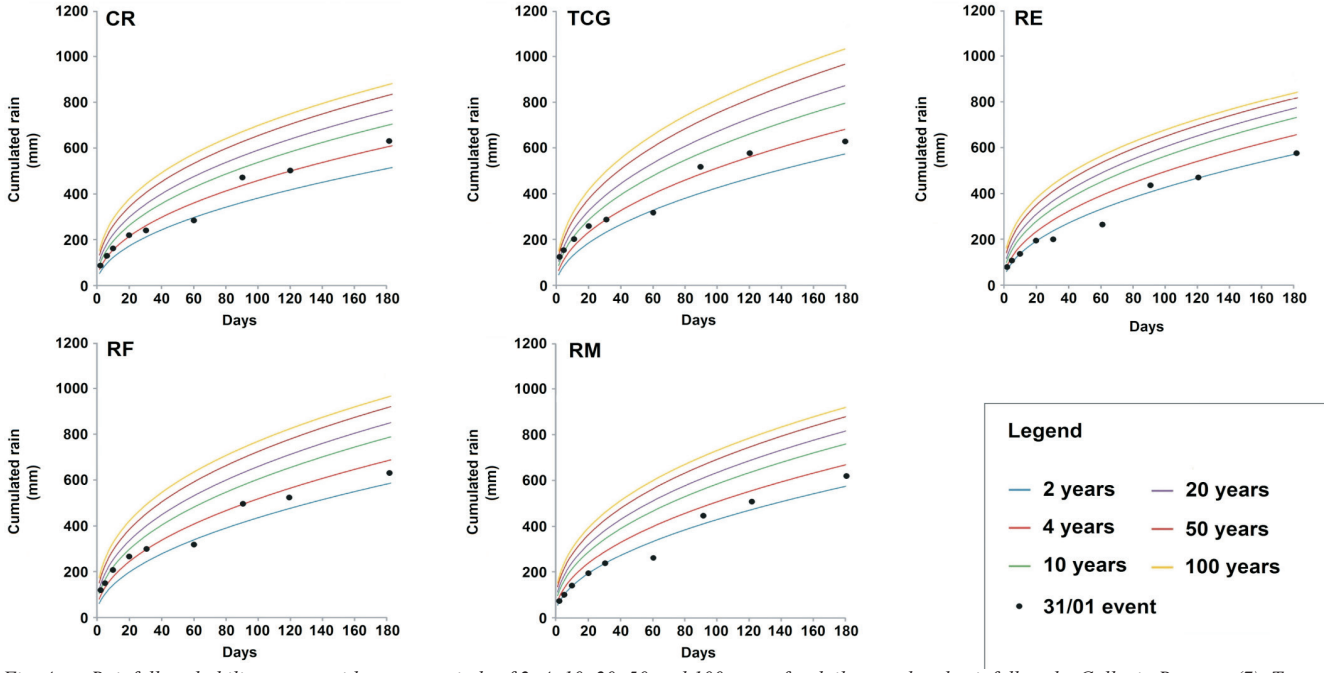

Fig. 4 - Rainfall probability curves with return periods of 2, 4, 10, 20, 50 and 100 years for daily cumulated rainfall at the Collegio Romano (7), Tevere Castel Giubileo (29), Roma Eur (16), Roma Flaminio (17) and Roma Macao (18) stations. The black dots denote the rainfall values recorded by the stations during the event of 31 Jan. 2014

Cumulated days	2		5		10		20		30		60		90		120		180	
Day/month	30/1	31/1	30/1	31/1	30/1	31/1	30/1	31/1	30/1	31/1	30/1	31/1	30/1	31/1	30/1	31/1	30/1	31/1
TCG	1	20	1	10	1	9	1	6	1	4	1	1	2	6	2	5	2	3
RF	1	15	1	8	1	8	1	6	1	4	1	1	2	4	1	3	2	3
CR	1	9	1	6	1	5	1	4	1	3	1	1	2	6	2	4	2	5
RM	1	3	1	2	1	2	1	2	1	2	1	1	2	3	2	3	2	3
RE	1	4	1	3	1	2	1	2	1	1	1	1	1	3	1	2	1	2

Tab. 2 - Estimated return periods (years) for rainfall cumulated in 2, 5, 10, 20, 30, 60, 90, 120 and 180 days prior to 30 Jan. and on 31 Jan. 2014

Their comparison suggests that, in this case, the rainfall values recorded by the Roma Flaminio and Tevere Castel Giubileo stations are lower than the ones of the other stations, especially in the range from 1 to 6 hours. This infers that, in the past, the intensity of hourly rainfall measured by the first two stations was lower than the one recorded by the other stations, contrary to what was observed on a daily basis. It is worth stressing, however, that data about intense precipitation are generally scantier than daily ones and that the resulting statistical analyses are usually less reliable. For instance, in this case, the stations of Roma Flaminio and Tevere Castel Giubileo recorded these data only for 26 and 25 years, whereas the Roma Macao, Roma Eur and Collegio Romano stations recorded them for 36, 35 and 32 years, respectively.

To estimate the return period of the event of 31 Jan. 2014, use was made of the rainfall probability curves pertaining to the intensity of 1-24 hours (Tab. 3).

The results show that, even on an hourly basis, the stations Roma Flaminio and Tevere Castel Giubileo have the longest return periods (especially for rainfall cumulated in 6 and more hours) whereas, at the other stations, the recorded event lay within the standard or quasi-standard range. Additionally, it is worth noting that the estimated return periods (in the range of 30 to about 100 years) are definitely longer for the hourly recorded event than for the daily recorded one, disregarding the previously described uncertainties.

In brief, statistical analyses validate the assumption that the

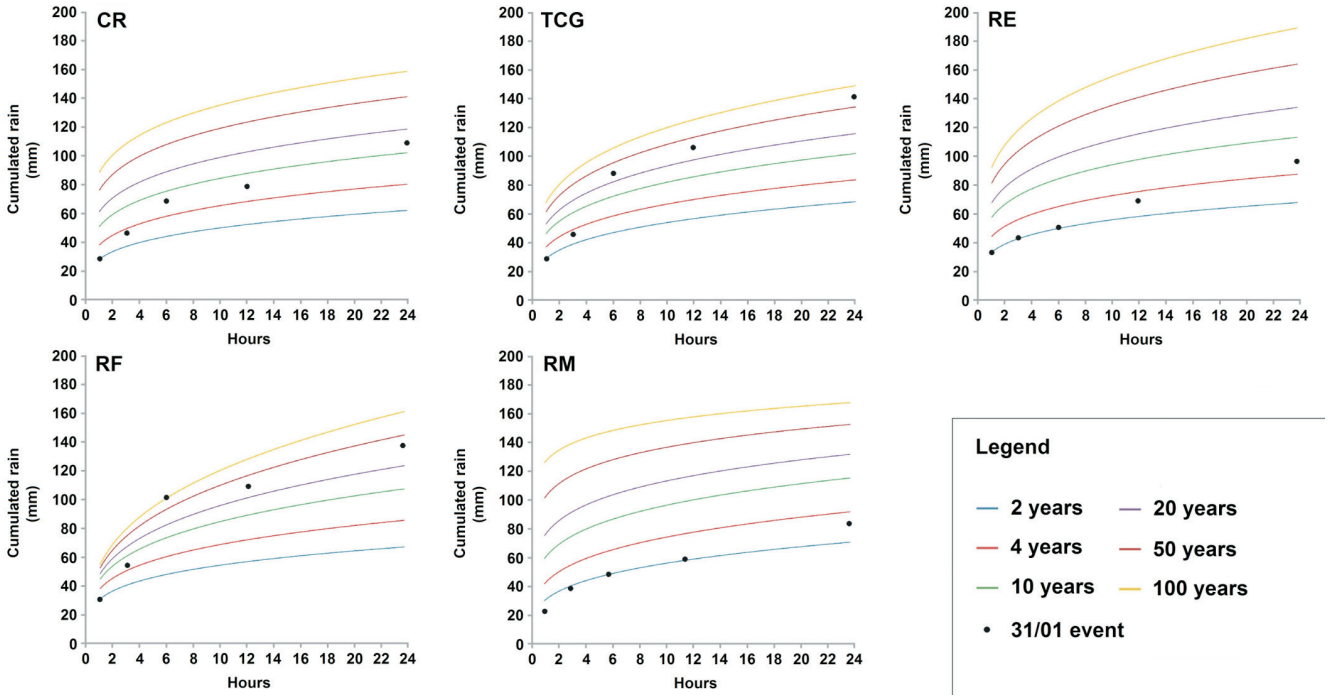

Fig. 5 - Rainfall probability curves with return periods of 2, 4, 10, 20, 50 and 100 years for hourly cumulated rainfall at the Collegio Romano (7), Tevere Castel Giubileo (29), Roma Eur (16), Roma Flaminio (17) and Roma Macao (18) stations. The black dots denote the rainfall values recorded by the stations during the event of 31 Jan. 2014

sector most severely stricken by the event of 2014 was also the one historically most prone to extreme rainfall (at least on the basis of daily records). Moreover, unlike the three other stations (at which the recorded event does not appear to be exceptional), the two most representative stations of the north-western sector are also those for which the longest return periods were calculated. This confirms that the event was extremely localised (as evidenced by areal rainfall) and particularly intense (especially in terms of rainfall cumulated in 6 and more hours).

ANALYSIS OF THE LANDSLIDES

Inventory

A detailed engineering-geological survey began in the morning of 31 Jan. and went on in the following 3 weeks. The survey collected qualitative and quantitative data on the landslides triggered by the exceptional rainfall that Rome experienced from 31 Jan. to 2 Feb. 2014.

The acquisition of field data (through systematic inspections) encompassed the direct observation of morphological and stratigraphic evidence, the collection of photographic material and the identification of the landslide location via GPS. The objectiveness of the collected dataset was checked by a comparative procedure, i.e. taking into account the data inventoried by different researchers for each landslide.

Cumulated Hours	1	3	6	12	24
Day/month	31/1	31/1	31/1	31/1	31/1
TCG	2	3	29	35	60
RF	2	6	102	30	31
CR	2	3	6	7	12
RM	1	2	2	2	3
RE	2	2	2	3	5

Tab. 3 - Estimated return periods (years) for rainfall cumulated in 1, 3, 6, 12 and 24 hours during the event of 31 Jan. 2014

The survey was conducted immediately after the critical rainfall event, to correlate it with the landslides identified and to investigate their original geomorphological features (see Plate I, section 5, for some examples).

Based on morphological evidence, the landslides were classified from the standpoint of their type of movement under the classification of Varnes (1978). Therefore, they were distinguished into falls, translational slides, rotational slides, earth flows, debris flows and complex slides. In places where human action had obliterated the

kinematic records of the triggering mechanism, the landslide was inventoried as "nd" (i.e. with an unclassifiable type of movement).

Out of the 68 landslides surveyed (Plate I, section 1), only 39 had such a size as to be mapped in detail (landslide body and estimated surface area). Among the landslides, 5 were classified as falls, 22 as rototranslational slides, 19 as translational slides, 5 as earth flows, 2 as debris flows, 11 as complex slides (Varnes; 1978) and 4 as not classified based on the collected observational data (Fig. 6)

All the landslides surveyed were differentiated into multiple lithological classes based on their dominant lithotypes (Tab. 4).

The graphs of Fig. 7 exhibit the results of the lithological distribution for each type of landslide, while the graph in Plate I, section 3 shows the percentage distribution of the landslide by geological formation.

A unique alphanumerical code was assigned to each of the landslides (alphabetical characters for the type of movement followed by a progressive number). For instance, the code RTR4 identifies rotational slide no. 4 (Tab. 5).

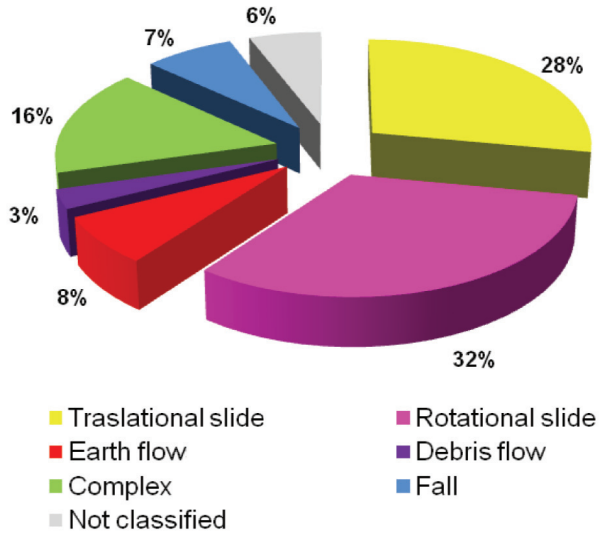

Fig. 6 - Percentage distribution of the 68 landslides inventoried in Rome's urban area after the exceptional rainfall of 31 Jan- - 2 Feb. 2014, by type of movement

Formation name (CARG 1:50000)	Abbreviation	Lithology	Lithologic class
Monte Vaticano Formation	MVA	Clay and Sand	B
Ponte Galeria Formation	PGLa	Sand - Sandy silt	A
Ponte Galeria Formation	PGL3a	Sand	A
Ponte Galeria Formation	PGL3b	Silty sand - Sand	A
Ponte Galeria Formation	PGL3c	Sand - Gravel	A
Monte Mario Formation	MTM	Sand	A
Farneto Member	MTM1	Sandy silt	C
Valle Giulia Formation	VGU	Sand	A
S. Cecilia Formation	CIL	Silt	C
Vitinia Formation	VTN	Silt	C
Tufi stratificati varicolori di Sacrofano	SKF	Tuff	E
Tufi stratificati varicolori di La Storta	LTT	Tuff	E
Slop Debris/Alluvial Deposits	SFTba	Sand	A
Anthropic fill	h	Anthropic fill material	F
n.a.	n.a.	Soil	D

Tab. 4 - Association of lithological classes and formational units from CARG (Carta Geologica d'Italia, 2008)

From 31 Jan. to 18 Feb. 2014, 68 landslides (most of which occurring from 31 Jan. to 7 Feb.) were inventoried.

The areal distribution of the landslides proved to be non-homogeneous within the area under review, since the landslides

ID	Type of landslide
CR	Fall
TR	Traslational slide
RTR	Rotational slide
CL	Earth flow
FD	Debris flow
COM	Complex

Tab. 5 - Relationship between landslide ID and landslide mechanism

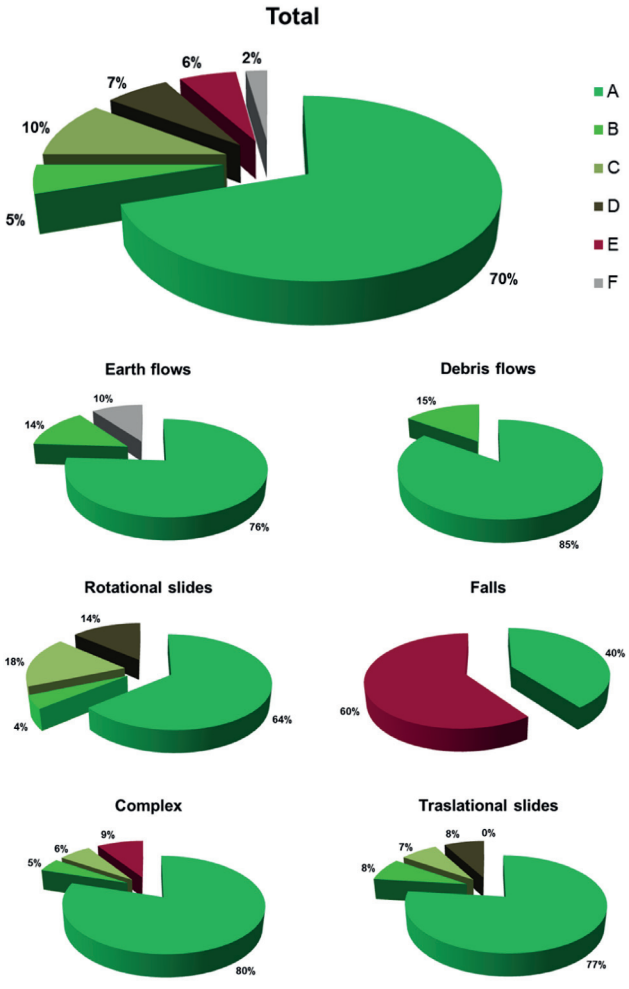

Fig. 7 - Percentage distribution of the 68 landslides inventoried in Rome's urban area after the exceptional rainfall of 31 Jan.- 2 Feb. 2014, by lithotypes involved and type of landslide

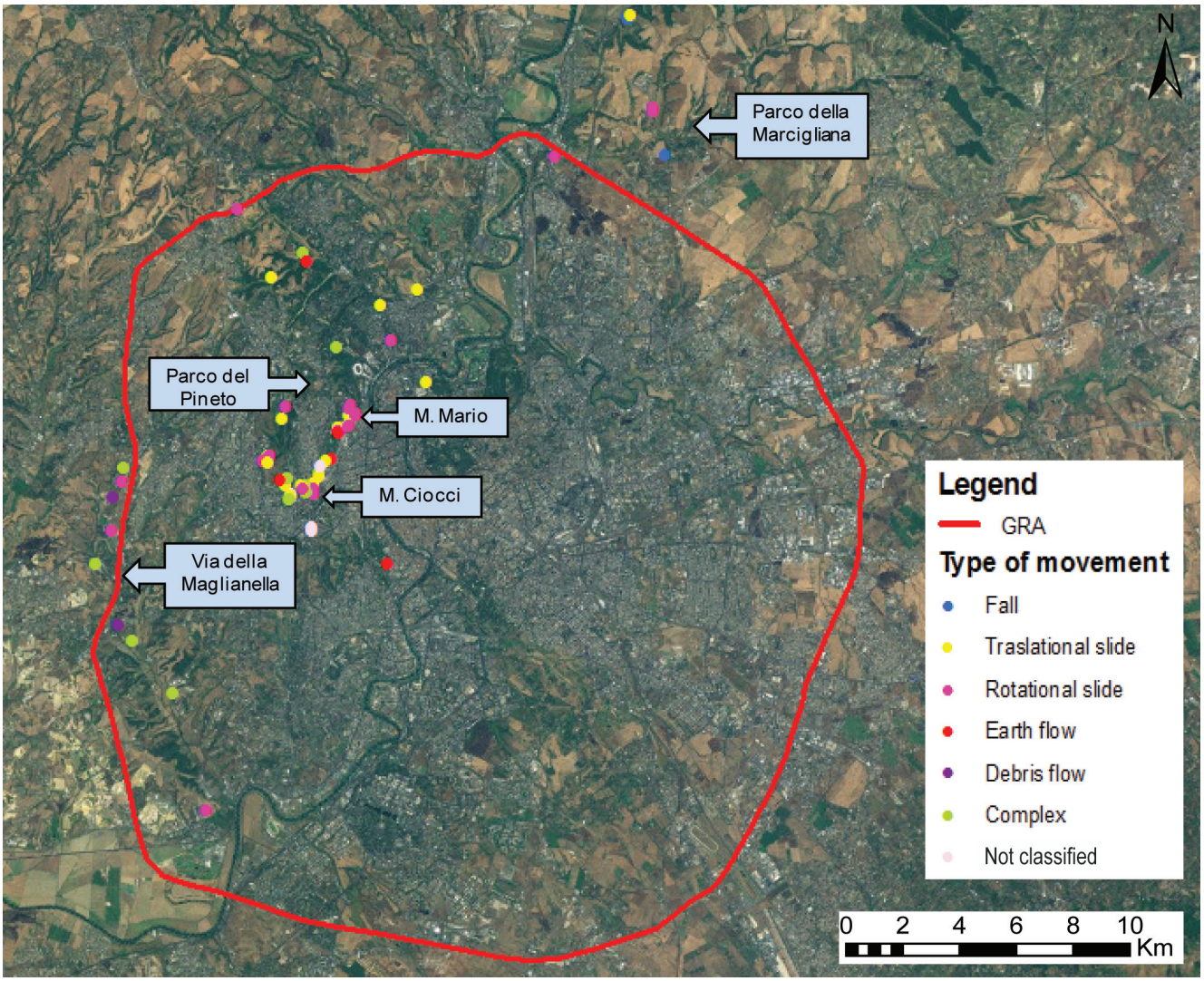

Fig. 8 - Location of landslides inventoried in Rome's urban area after the exceptional rainfall of 31 Jan- - 2 Feb. 2014; each of them is associated with a unique alphanumerical code. The landslides are colour-coded based on their mechanism of rupture

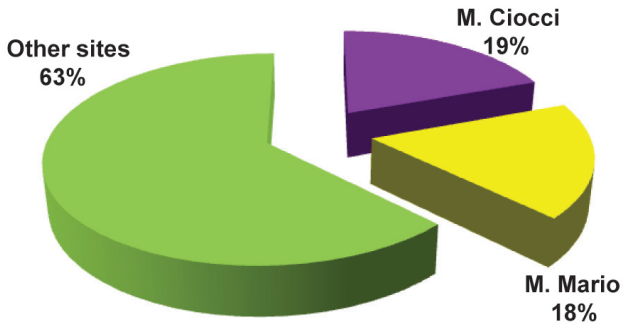

Fig. 9 - Statistical analysis of the 68 landslides inventoried. Distribution of the number of landslides detected at Monte Ciocci (purple), Monte Mario (yellow) and in the remaining urban area of Rome (green)

were concentrated in the north-western part of Rome (Fig. 8).

The reliefs of Monte Mario and Monte Ciocci (Fig. 9) had a high concentration of landslides: 25 of the 68 landslides inventoried, i.e. over 30% of the total. In particular, 12 slides affected the SE slope of Monte Mario, while 13 occurred on the SE and SW slopes of Monte Ciocci.

Most of these slides were translational and rotational and involved relatively shallow portions of the slopes, consisting of man-made fills and non-volcanoclastic lithotypes, mostly clayey, from the *Monte Vaticano Formation*. To a lesser extent, they affected dominantly sandy deposits belonging to the *Monte Mario Formation* and to the conglomeratic lithofacies of the *Ponte Galeria Formation (Monte Ciocci unit Auctt.*) (Fig. 10a).

By contrast, the landslides spared the hills located on the left bank of the Tiber; the only exception was the western slope of the

Villa Glori hill, which had a translational slide of limited extent involving sandy travertine deposits from the *Valle Giulia Formation*.

Another area with landslides induced by rainfall was the western portion of Rome's urban area, along Via della Magliana and Via della Maglianella (Fig. 10b). Here, 10 landslides occurred within dominantly sandy sedimentary deposits. Among them, a debris flow involved sandy silts presumably belonging to the *Ponte Galeria Formation*.

Numerous landslides were also observed inside "urban parks", including Parco del Pineto and Riserva Naturale della Marcigliana (Marcigliana nature reserve). At Parco del Pineto, the landslides were shallow and of limited extent and originated inside sandy-silty deposits with thin intercalations of gray clay ascribed to the *Ponte Galeria Formation.* Some slides at the Riserva Naturale della Marcigliana unusually affected the tuff cliffs belonging to the *Tufi Stratificati Varicolori di La Storta Formation*. In particular, the translational slide "TR10", involving in part the soil and in part the debris generated by tuff weathering, invaded the roadway of Via della Marcigliana, which was thus closed to vehicle traffic (Fig. 11).

Fig. 10 - Examples of landslides triggered in Rome by the exceptional rainfall event of 31 Jan.-2 Feb. 2014: a) complex side along Via Simone Simoni (Monte Ciocci); b) rotational slide along Via della Maglianella

The remaining landslides were more unevenly distributed in the urban area of Rome and anyway ever in its northern quadrant, as in the case of the landslide on the slope along the inner lane of the Grande Raccordo Anulare (GRA) ring road, the one along Via del Foro Italico and the falls observed along Viale Tiziano, which involved cemented sands supposedly belonging to the *Valle Giulia Formation*.

Most of the landslides were classified as dominantly rotational and subordinately translational (Tab. 6). Rotational slides also had the largest areal extent, even if the most extensive slide "TR7" (occurred along Via S. Simoni on the south-eastern side of Monte Ciocci on 31 Jan., see Plate I, section 5A) had a translational kinematics. It should be pointed out that the areal data shown in Tab. 6 and in the graphs do not refer to all of the landslides, but only to those extending over a surface area of more than 35 m^2 (39 landslides).

The numerous slope instabilities identified may be classified as shallow slides, in that their maximum depth (rotational slide of Via Cavalieri di Vittorio Veneto "RTR15", see Plate I, section 5D) is about 5 m, whereas most of the landslides are less than 1

Fig. 11 - Examples of landslides triggered in Rome by the exceptional rainfall event of 31 Jan.-2 Feb. 2014: translational slide along Via della Marcigliana

Type of lanslide	N. events	A_max (m^2)	A_av (m^2)	A_tot (m^2)
Fall	5	-	-	-
Traslational slide	19	4970	763	8400
Rotational slide	22	4120	11150	14953
Earth flow	5	350	220	670
Debris flow	2	2300	1300	2600
Complex	11	4800	924	9240

Tab. 6 - Number of landslides and their surface area (maximum - max; average - av; total - tot) by type of mechanism of rupture. The analysis was conducted on the 39 mappable landslides

m deep. Due to the limited thickness of the landslide masses, they are generally constituted of weathered soils. To exemplify the physical and mechanical properties of the weathered soil layers involved in the landslides on the Monte Mario hill, some undisturbed samples were obtained from the main scarp of the aforementioned landslide "RTR15". These samples were tested at the laboratory of "Geologia Applicata" of the Department of Earth Sciences, University of Rome "Sapienza". As indicated by lab tests, the sampled soil is a weathered silty-clayey mixture classified as CL under the USCS classification (ASTM D2487, 2010). Lab-determined values are as follows: solid weight per unit volume (ASTM D854, 2010) 26.22 kN/m^3; natural water content (ASTM D2216, 2010) 25.7%; plastic and liquid Atterberg limits (ASTM D4318, 2010) 22.9% and 40.1% respectively, and mineralogical activity 0.31. Direct shear tests (ASTM D3080, 2004) yielded: a value of 27° for the internal friction angle corresponding to the peak shear strength; a drained cohesion of about 20 kPa, and a value of 25° for the internal friction angle corresponding to the residual shear strength. Furthermore, based on in-situ tests performed by the Municipality of Rome in the same landslide area, the undrained cohesion is of about 300 kPa.

In spite of their limited surface area, 40% of the landslides

Fig. 12 - Examples of damage caused in Rome by the landslide triggered by the exceptional rainfall event of 31 Jan.- 2 Feb. 2014: a) rototranslational slide of Via del Foro Italico (Tangenziale nord), detail of damage to the low wall bordering the roadway; b) rototranslational slide along Via Cavalieri di Vittorio Veneto, which was then closed to vehicle traffic; c) translational slide on the eastern side of Monte Ciocci along Via S. Simoni; d) detail of damage caused by the landslide along Via S. Simoni to the roofed car parks

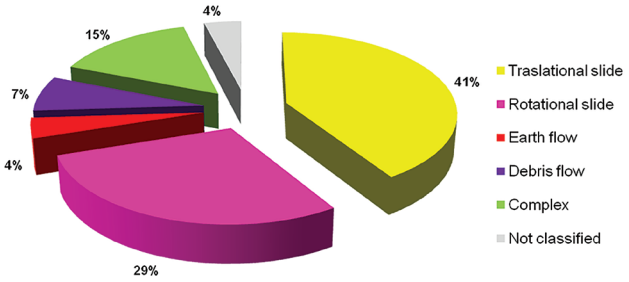

Fig. 13 - Percentage of damage associated with each mechanism of rupture

caused major damage. Most of them posed a high risk to buildings and infrastructures of critical importance to urban transport.

In particular, at Monte Mario, the rotational slides of Via Trionfale "RTR16" (see Plate I, section 5D) and of Via Cavalieri di Vittorio Veneto "RTR15" (Fig. 12b) disrupted transport routes and made it necessary to evacuate some buildings from 8 Feb. on. Among the landslides arising on the eastern side of Monte Ciocci, two caused damage to buildings: the complex landslide "COM1" (Fig. 12a) and the translational slide "TR7" made some roofed car parks inaccessible owing to the accumulation of material (Fig. 12c-d).

Along Via Cassia, in the section extending from Piazza dei Giuochi Delfici to Via Pareto, the shallow translational landslide "TR16" involved the weathered layer of the *Valle Giulia Formation*, invading the roadway that was subsequently protected by jersey barriers.

The landslides that caused the most serious damage to transport routes, especially to high-speed roads, took place near Via del Foro Italico ("RTR12") and along the GRA ring road near Casal del Marmo ("RTR14") on 31 Jan. The rotational landslide "RTR12" (Fig. 12a) affected sands, sandy silts and man-made fills over an area of approximately 320 m^2, entailing the collapse of the retaining wall bordering the roadway and the pouring of part of the landslide debris onto the roadway. Also the landslide that occurred along the GRA had a rototranslational mechanism of rupture and involved silty-sandy deposits. The detachment area extended over about 160 m^2, whereas the slide material, filling the inner lane of the GRA, disrupted road traffic but caused minor structural damage to the retaining wall bordering the roadway. Furthermore, multiple scarps with a height of about 50 cm were detected in the area uphill of the landslide, pointing to a possible retrogressive mechanism.

A quantitative analysis of the damage caused by the different slides, based on the inventory discussed here, evidences that translational landslides were responsible for 41% of the damage (11 slides), rototranslational landslides for 29% (8 slides), whereas the remaining types of movement caused less than 15% of the damage. It is worth emphasising that the falls did not induce infrastructural damage (Fig. 13).

All the collected data were fed to a geodatabase (see Plate I, section 4) and managed, queried and processed in a GIS environment. Finally, they were implemented as metadata in accordance

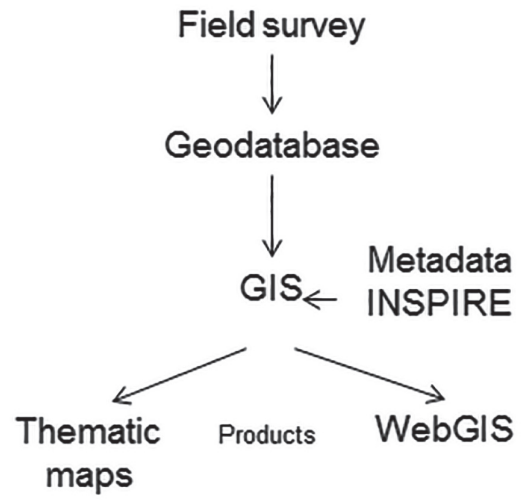

Fig. 14 - Workflow for implementing the geodatabase and the related queries via WebGIS

with the INSPIRE (INfrastructure for SPatial InfoRmation in Europe) Directive.

The deliverables from the project of identification, characterisation and classification of the landslides observed in Rome's urban area consist of: detailed thematic maps (scale 1:1,000), subsequently projected onto the topographic base CTR 1:5000 of the Latium region, and of the on-line WebGIS inventory posted on CERI website (www.ceri.uniroma1.it).

At each stage of the research project (Fig. 14), the instability data were validated by systematically checking whether the elements viewed in the GIS environment matched the data collected during field surveys.

The geodatabase is made up of different tables and feature-classes, interconnected by key fields (e.g. the unique identifier of the landslide, ID) through one-to-many and one-to-one relations, which return the data associated with the landslide, e.g.: date of observation, photographs, location and geographic coordinates in WGS84 UTM 33N, mechanism of rupture and morphometric features (namely, height of the main scarp, width and length of the landslide body). Furthermore, for each landslide, the geodatabase describes the lithotypes involved and the belonging "formation" reported in the official geological map, Sheet Roma 374, scale 1:50,000 (Funicello & Giordano, 2008). The database also specifies whether the landslide caused or did not cause damage to buildings and structures and the type of damage (Tab. 7).

The distribution of the landslides generally confirmed the one reported in official inventories (AVI, IFFI, PAI, PRG) that identify the centres of landslides in Rome's urban area in the morphological highs and hillsides of the valleys, carved by the stream network see Plate I, section 1).

The "Piano Regolatore Generale" (master land-use plan) of

ID	Lat	Long	Location	Date	Lithology	Formation	Water	Type of landslide	Scarp height (m)	Length (m)	Width (m)	Damages
CL1	4643165,900	288312,457	Via Labriola	07-feb-14	sand	PGLa	no	Earth flow	0,5	35	10	yes
CL4	4642621,279	286989,238	Parco del Pineto	13-feb-14	sand	PGLa	nd	Earth flow	0,5	8	3	no
CL5	4640421,771	289809,368	Via Garibaldi	10-feb-14	sand	MTM	no	Earth flow	1	1	4	yes
CL6	4643890,207	288510,3315	Via Trionfale	13-feb-14	sand	MTM	yes	Earth flow	1	20	7	no
CL7	4648415,570	287659,56	Insugherata	25-feb-14	sandy silt	MTM	nd	Earth flow	0,5	20	14	no
COM1	4642793,299	288001,416	Via S. Simoni	07-feb-14	clay and sand	PGLa - MVA	yes	Complex	2	40	60	yes
COM11	4642079,412	287215,5573	Via Moricca	07-feb-14	nd	SKF - LTT	yes	Complex	1	70	60	yes
COM12	4648648,960	287566,59	Insugherata	25-feb-14	sand	MTM	nd	Complex	2	60	23	no
COM13	4642500,680	287613,94	Monte Ciocci	25-feb-14	sandy silt	PGLa	nd	Complex	1,5	5	4	no
COM14	4646123,240	288448,17	Valle Farneto	25-feb-14	sand	MTM	nd	Complex	1	10	15	no
COM2	4642309,447	287661,034	Via di Valle Aurelia	07-feb-14	sand	PGLa	no	Complex	1,5	20	80	yes
COM4	4640413,258	282101,361	Via Aurelia	08-feb-14	sand	PGL3b	yes	Complex	3	20	40	yes
COM5	4642968,481	282859,755	Maglianella	08-feb-14	sand	PGL3b	yes	Complex	3	30	6	no
COM6	4638356,604	283075,018	Via Brava	08-feb-14	sand and gravel	PGL3b	yes	Complex	1	12	16	no
COM7	4636992,200	284166,068	Via Pnt. Pisano	08-feb-14	sand and gravel	PGL3c	no	Complex	1	10	15	no
COM8	4642675,247	287176,324	Parco del Pineto	13-feb-14	sand	PGLa	yes	Complex	0,5	50	80	no
CR1	4651216,574	297138,062	Via Bufalotta	08-feb-14	tuff	LTT	yes	Fall	0,5	3	4	no
CR2	4654853,798	296139,927	Via Bufalotta	08-feb-14	tuff	LTT	no	Fall	0,5	5	4	no
CR3	4654891,535	296149,301	Via Bufalotta	08-feb-14	tuff	LTT	no	Fall	0	0	0	no

Tab. 7 - Database report

Rome/2007 (Carta di vulnerabilità geologica del territorio comunale - map of geological vulnerability of the municipal area) shows areas historically affected by landslides. The plan indicates that 56% of the landslides triggered by the rainfall event of 31 Jan. 2014 developed in areas previously classified as unstable.

In particular, in the map of geological vulnerability of the municipal area, the SE slopes of Monte Mario and Monte Ciocci feature a wide belt that is prone to gravitational deformations. Consequently, the landslides observed along Via Cavalieri di Vittorio Veneto - Via Trionfale are located in an area already mapped as "landslide-prone".

As regards the earth flow recently reactivated on the slope of Monte Ciocci along Via Labriola, the first documented activation leads back to 1960 and required the evacuation of 60 people, whereas the latest one occurred in 1998, when the translational slide evolved into an earth flow that damaged the retaining wall bordering the road (Amanti *et alii*, 2008). Also the complex slide, detected on the SE side of Monte Ciocci along Via S. Simoni, is the reactivation of a historical landslide occurred in December 2008 (Amanti & Fabbri, 2014).

The falls observed along Viale Tiziano occurred in an area historically susceptible to this type of gravitational movement. Bibliographic sources of the 1930s report the evolutionary trend of the travertine walls of Viale Tiziano, with falls and accumulation of material downslope (De Angelis D'Ossat, 1932). The main event mentioned in the databases of AVI and IFFI is the one of 1972, which mobilised about 500 m^3 of soil. This event was induced not only by geological and geomorphological predisposing factors, but also by anthropogenic action that changed the gradient of and the stresses within the slope (Amanti *et alii*, 2008). The latest activation on the slope of Viale Tiziano took place in November 2007 and was very similar to the reactivation of 1972 (Amanti *et alii*, 2012) and to the landslide recorded in February 2014.

Landslides distribution analysis

A morphometric analysis of the 68 landslides was conducted on the cartographic base onto which the field surveys had been projected. The analysis made it possible to map the statistical distribution of the landslides vs. their surface area and the gradient of the slope involved. The analysis took into consideration only the 39 landslides whose areal extent could be mapped.

The diagrams of Fig. 15 show these distributions, divided by size of the landslide: Fig. 18a (left) refers to all of the landslides, while Fig. 15b (right) concerns only those extending for more than 1,000 m^2 (about 25% of the total). Though Fig. 15a shows an apparently random distribution, Fig. 15b evidences a correlation between the gradient of the slope and the size of the process.

Then, a weighted landsliding index (IF%) was calculated. This index is given by the percentage ratio of the landslide area for each lithotype to the total landslide area (Tab. 8). The index was calculated only for the 39 landslides whose areal extent could be determined.

	Sand	Clay	Silt	Soil
Outcropping area (m^2)	24195	453	4538	6758
IF (%)	67	1	13	19

Tab. 8 - Explanatory table of the weighted landslide susceptibility index (IF %)

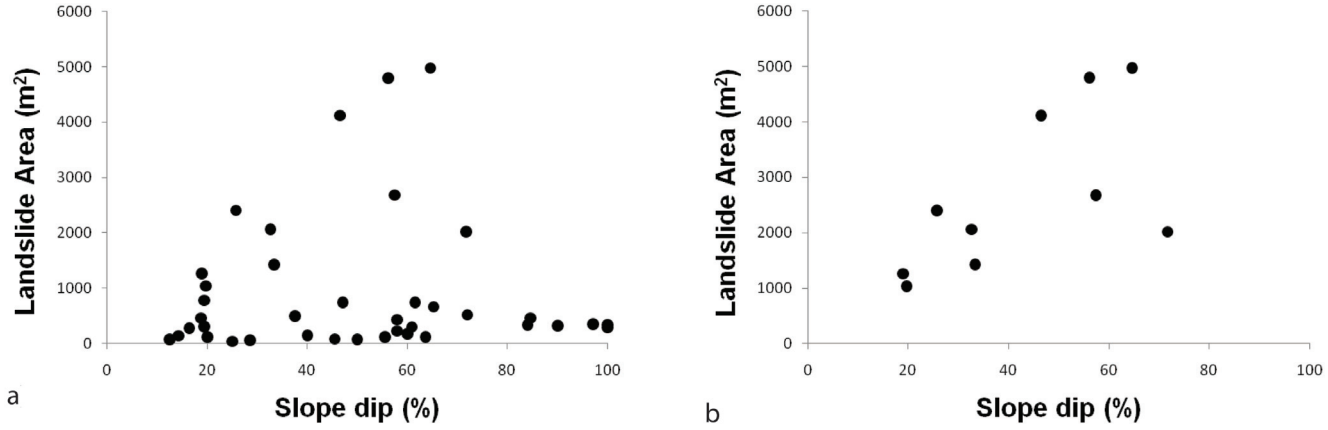

Fig. 15 - Distribution of the landslides (areal extent vs. relative slope gradient): a) all landslides, b) only landslides having an areal extent of more than 1,000 m. The analysis was made on the 39 mappable landslides

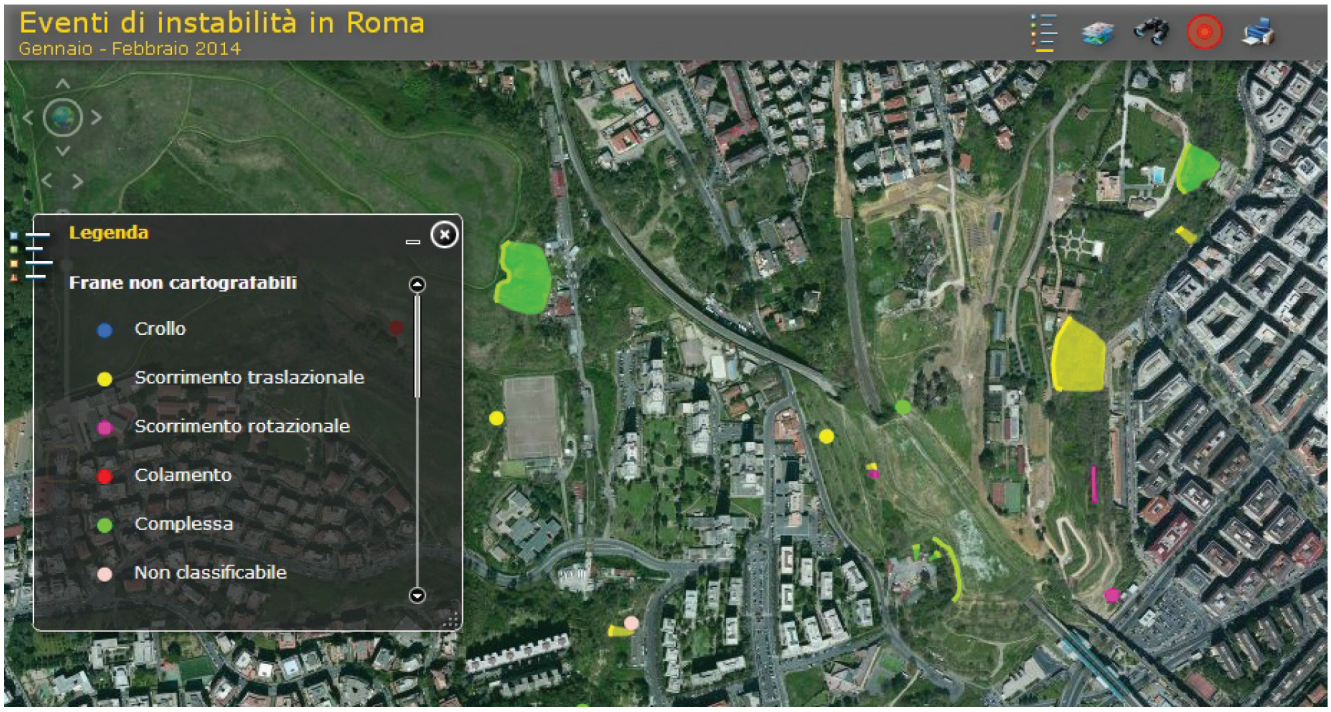

Fig. 16 - On-line WebGIS: example of simplified geomorphological map using different colours

WebGIS inventory

The WebGIS for the inventory discussed in this paper has been made publicly available on CERI's website (www.ceri.uniroma1.it), in the WebGIS section, since 9 May 2014. Users may view the location of the landslides and the related geomorphological maps.

The nature of the queryable data depends on the viewing scale: for scales of up to 1:10,000, the events are displayed as dots with respect to the centroids of the landslide body. At smaller scales, the geomorphological maps are divided into areal and linear forms of landslides with a minimum mappable extent. The use of different colours for geomorphological symbols makes it possible to identify the type of mechanism of rupture, described by an appropriate legend (Fig. 16).

The WebGIS offers different query options: free text search, by address or geographic coordinates (latitude, longitude), and guided search, by type of movement or merely by delineating the area of interest on the map (Fig. 17).

By pressing "stampa" (print), the data of the map may be printed in .pdf format or as images in different formats.

Each level that the user may select, by a single click of the

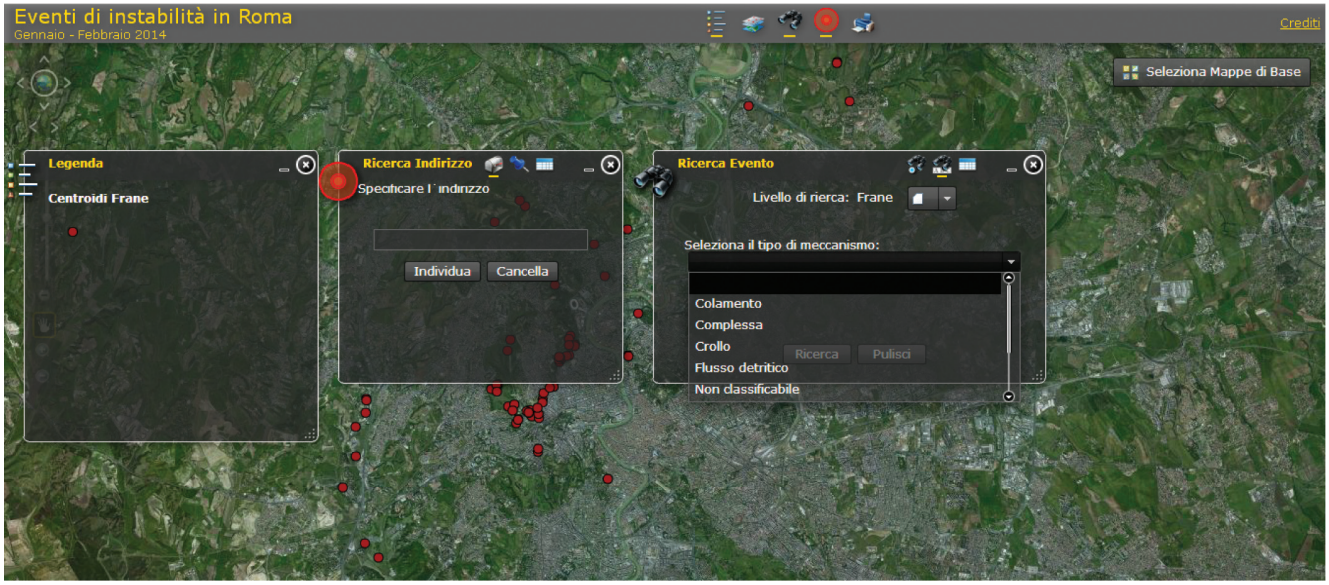

Fig. 17 - On-line WebGIS: query windows for guided search and related options

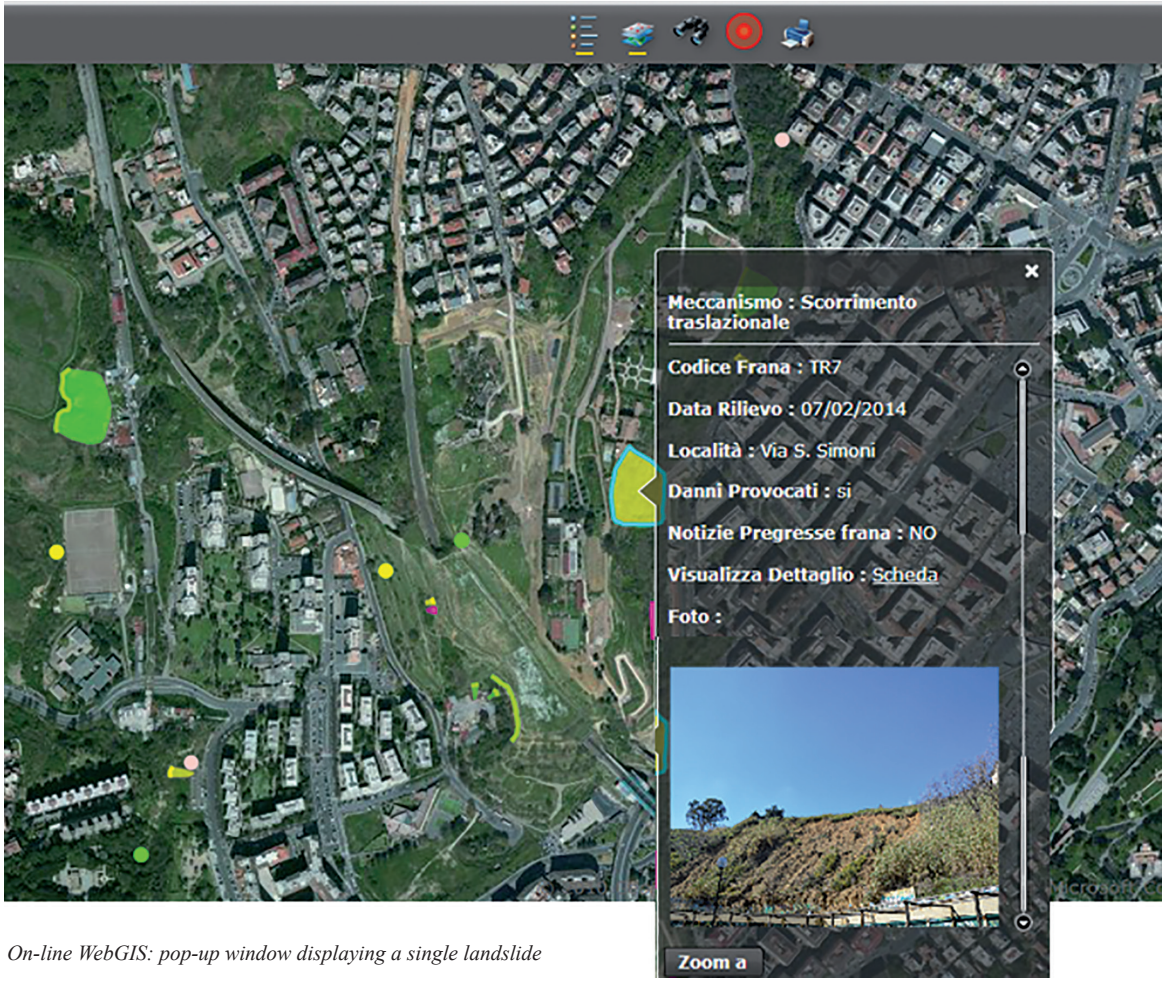

Fig. 18 - On-line WebGIS: pop-up window displaying a single landslide

mouse or via the search option, is associated with a pop-up window; this window displays the basic data of the landslide, e.g. ID of the event, mechanism of rupture, location, lithotype involved and belonging geological formation (according to the legend of Sheet 374 of Funicello & Giordano, 2006), as well as a photograph of the landslide.

The pop-up window also comes with: a link to a detailed datasheet of the landslide, with the morphometric data collected in the field (Fig. 19); a wider description of the phenomenon; photographs; an except from the official geological map (Funicello & Giordano, 2006) to a scale of 1:10,000, and a geomorphological map to a scale of 1:1,500.

DISCUSSION

An analysis was made of the spatial distribution of the rainfall event that triggered landslides in Rome between the end of January and the beginning of February. The analysis reported herein highlights the non-homogeneous distribution of the event, since it mostly affected the NW portions of the urban area, especially the slopes of Monte Mario and Monte Ciocci, and caused the highest number of landslides just in that area (Fig. 20).

In view of the above, it might be assumed that the spatial distribution of the phenomenon was affected by local orography and that the heavy rainfall originated from the ascent of air masses

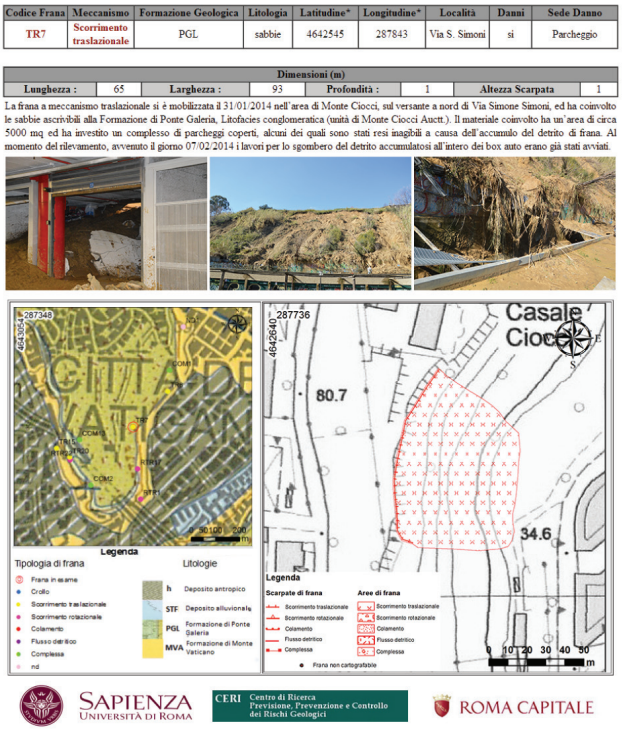

Fig. 19 - On-line WebGIS: detailed technical schedule of a single landslide

along the eastern foot of the hills. This phenomenon might have decreased the temperature of air moving uphill at Monte Mario and Monte Ciocci, making it water vapour-saturated and inducing condensation and precipitation. Nevertheless, considering an average adiabatic temperature decrease (vertical thermal gradient) of 1°C/100 m of ascent along the hills (Pinna, 1977) and the small elevation of Rome's hills (Monte Mario 144 m and Monte Ciocci 77 m above sea level), the orographic cause of the concentrated rainfall that lashed the north-western portions of the city can be ruled out. Indeed, the small elevation of the hills does not permit water vapour to reach saturation.

Hence, it is more realistic to take into account weather conditions at a wider scale, i.e. the weather conditions of Italy on 31 Jan. 2014, the day with the maximum intensity of rainfall.

The high number of landslides that ravaged Rome from 31 Jan. 2014 to 7 Feb. 2014 is thus related to its particular weather conditions, which led to an exceptional concentration of the intensity of hourly rainfall (return period of rainfall cumulated in

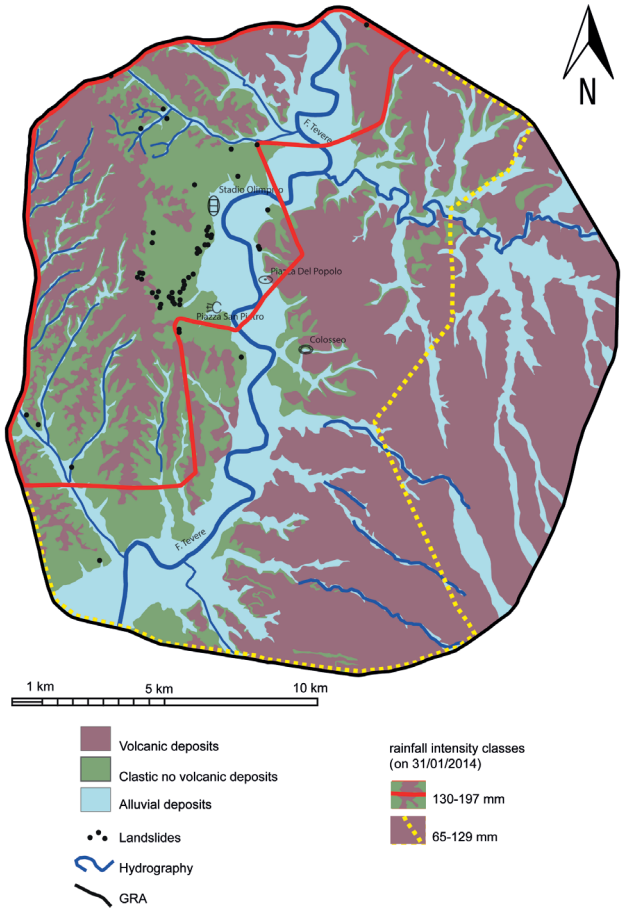

Fig. 20 - Lithological map of the city of Rome, with the location of the inventoried landslides and the distribution of rainfall on 31 Jan. 2014 - Thiessen polygon method

6 hours: 100 years) and not of the intensity of daily rainfall (unexceptional return periods of roughly 20 years). In fact, given its meridian direction, the storm system mostly affected the non-volcanoclastic deposits that oucrop near the reliefs along the right bank of the Tiber (especially those of Monte Mario and Monte Ciocci). These deposits are particularly prone to instabilities owing to their geomorphological setting (steep slopes) and to the strong anthropogenic pressure that they experienced in the second half of last century (Bozzano *et alii*, 2006). Moreover, their prevalently clayey-silty or sandy nature generally makes them more susceptible to landslides induced by intense precipitation. The analysis of the landslide distribution, carried out as part of the research project and focused on the event occurred from 31 Jan. to 7 Feb. 2014, shows that 69% of the phenomena developed inside dominantly sandy and sandy-silty deposits (*Monte Mario, Ponte Galeria, Valle Giulia Formations*) and only 6% inside the "Tuffs" from the Sabatini Mts. volcanic district.

By contrast, the inventory of historically documented landslides (Amanti, 2008) demonstrates that most of them (dominantly falls) involved the southern sector of Rome, namely volcanic deposits from the Alban Hills volcanic district. In effect, the inventory indicates that 41% of the landslides reported in Rome involve "tuffs" and "pozzolanas" and only 1.7% dominantly sandy deposits, e.g. those ascribable to the *Monte Mario, Ponte Galeria* and *Valle Giulia Formations*. Based on the findings from this study, this apparent statistical anomaly may be due to three main factors: 1) spatial distribution of rainfall, confined to the NW zone of Rome's urban area; 2) non-homogeneous geological setting of the hills located on the right and left banks of the Tiber; 3) higher topographic elevation of reliefs on the right bank of the Tiber.

CONCLUSIONS

The analysis of the landslides triggered in Rome by the exceptional rainfall of late January-early February 2014 showed an abnormal statistical distribution vs. the one of historical landslides. The anomaly was correlated with: i) the distribution of rainfall cumulated in 6 hours, which represented an exceptional episode with a return period of more than 50 years; ii) the dominant involvement of the NW sector, whose hills have more differences in height than other sectors of the urban area, and iii) the occurrence in such sector of dominantly non-volcanoclastic deposits.

Such anomaly highlights the importance of reconstructing triggering scenarios, with a view to predicting the spatial distribution and types of triggered landslides (trigger-controlled statistics), rather than relying on general data provided by medium-long term statistics. Indeed, the latter data disregard the triggers, placing greater emphasis on the role of landslide predisposing factors (proneness-controlled statistics).

All this stresses the potential value for the city of Rome of modelling and quantifying specific hazard scenarios, so as to address geological risks in urban areas and pursue city management policies aimed at mitigating their effects and damage.

ACKNOWLEDGMENTS

The authors thank: Roma Capitale and, in particular, Ignazio Marino (Mayor), Paolo Masini (member of the municipal government in charge of "Sviluppo delle periferie, infrastrutture e manutenzione urbana" - development of outskirts, infrastructure and urban maintenance), Maurizio Pucci from "Direzione Promozione, pianificazione strategica e coordinamento attuativo di progetti speciali, per lo sviluppo e la valorizzazione della città di Roma e le sue risorse" - department of promotion, strategic planning and coordination of the implementation of special projects for enhancing the value of Rome and its resources), for their logistic support; the technical specialists from the Municipality of Rome, Maurizio Allevi, Angelo Canalini, Mariachiara Galiano, Fabrizio Mazzenga, Theo Uber, for their technical support; Stefano Casini, Giuseppe De Pisa, Fabrizio Foschi from Roma Natura, for providing data and technical support in the areas of the urban parks; Andrea Luzzi Franzoni from the "Centro funzionale della protezione civile della Regione Lazio" (functional civil protection centre of the Latium region), for providing data on and interpretations of the rainfall event discussed in this paper.

REFERENCES

Alvarez W., Ammerman A.J., Renne P.R., Karner D.B., Terrenato N. & Montanari A., (1996) - *Quaternary fluvial-volcanic stratigraphy and geochronology of the Capitoline hill in Rome*. Geology, **24**: 751-754.

Amanti M., Cesi C. & Vitale V. (2008) - *Le frane nel territorio di Roma (ed) "La Geologia di Roma"*. Memorie Descrittive della Carta Geologica d'Italia, **80**: 83-117.

Amanti M., Chiesi V. & Guarino P.M. (2012) - *The 13 November 2007 rock-fall at Viale Tiziano in Rome (Italy)*. Nat. Hazards Earth Syst. Sci., **12**: 1-12.

Amanti M. & Fabbri M. (2014) - Convenzione Protezione Civile Roma Capitale - Ordine dei Geologi del Lazio e Progetto Pilota Comune di Roma - ISPRA - OGL. 11 febbraio 2014. *http://geologilazio.it/public/file/2014/03/Amanti_Fabbri_prot_civile.pdf*

Anzidei M., Carapezza M.L., Esposito A., Giordano G., Tarchini L. & Lelli M. (2008) - *The Albano Maar Lake high resolution bathymetry and dissolved CO_2 budget (Colli Albani District, Italy): constrains to hazard evaluation*. J. Volcanol. Geotherm. Res., **171**: 258-268.

Archivio Previsioni Meteorologiche CNR-ISAC. *http://www.isac.cnr.it/dinamica/projects/forecasts/moloch/*

Ascani F., Bozzano F., Buccellato A., Del Monte M., Matteucci R. & Vergari F. (2008) - *Evoluzione del paesaggio e antiche vie di drenaggio nell'area*

de "Il Castellaccio" (Roma) da indagini geologiche, geomorfologiche e archeologiche. Geologica Romana **41**: 55-77.

ASTM D2487 (2010) - *Standard Practice for Classification of Soils for Engineering Purposes (Unified Soil Classification System)*. 3-5.

ASTM D854 (2010) - *Standard Test Methods for Specific Gravity of Soil Solids by Water Pycnometer*, 2.

ASTM D2216 (2010) - *Standard Test Methods for Laboratory Determination of Water (Moisture) Content of Soil and Rock by Mass.* 1-5.

ASTM D4318 (2010) - *Standard Test Methods for Liquid Limit, Plastic Limit, and Plasticity Index of Soils*. **1**.

ASTM D3080 (2004) - *Standard Test Method for Direct Shear Test of Soils Under Consolidated Drained Condition*. pp. 1-3.

Various Authors (2011) - *La pericolosità sismica nel Lazio.* A cura di Scarascia Mugnozza G. Quaderni dell' "Italian Journal of Engineering Geology and Environment", **4.**

AVI (1996) - *Aree vulnerate italiane.* A cura di Coordinamento della Protezione Civile al Gruppo Nazionale per la Difesa dalle Catastrofi Idrogeologiche (GNDCI) del Consiglio Nazionale delle Ricerche (CNR). *http://avi.gndci.cnr.it*

Basili R., Valensise G., Vannoli P., Burrato P., Fracassi U., Mariano S., Tiberti M.M. & Boschi E. (2008) - *The Database of Individual Seismogenic Sources (DISS), version 3: summarizing 20 years of research on Italy's earthquake geology.* Tectonophysics, DOI:10.1016/J.TECTO.2007.04.014

Bencivenga M., Di Loreto E. & Liperi L. (1995) - *Il regime idrologico del Tevere, con particolare riguardo alle piene nella città di Roma*. Memorie descrittive della Carta Geologica d'Italia, **50:** 125-172.

Bozzano F., Giacomi A.C., Martino S., C.P.VV.F. Roma (2011) - *Scenari di danneggiamento indotto nella città di Roma dalla sequenza sismica aquilana del 2009*. Italian Journal of Engineering Geology and Environment, **11(2)**: 5-22.

Bozzano F., Martino S. & Priori M (2006).- *Natural and man-induced stress evolution of slopes: the Monte Mario hill in Rome*. Environmental Geology, **50(2)**: 505-524.

Carapezza M.L., Badalamenti B., Cavarra L. & Scalzo A. (2003) - *Gas hazard assessment in a densely inhabited area of Colli Albani Volcano (Cava dei Selci, Roma)*. J. Volcanol. Geotherm. Res. **123**: 81-94.

Castiglione L., Coppola G., D'Armento E. & Rosso F. (2014) - *Gli eventi franosi ed alluvionali del 31 gennaio 2014 a Riano (Roma)*. Professione Geologo, **39**: 10-14.

Centro Funzionale Regione Lazio (2014) - *Rapporto di evento del 31 gennaio - 04 febbraio 2014*: 41

Cifelli F., Donati S., Funiciello F., Gasparini C., Saraceni A. & Tertulliani A. (1997) - *Il risentimento a Roma del terremoto umbro-marchigiano del 14 ottobre 1997*. Proceedings of XVI CNR-GNGTS, 11-13 November 1997, Roma

Ciotoli G., Etiope G., Florindo F., Marra F., Ruggiero L., Sauer P.E. (2013) - *Sudden deep gas eruption nearby Rome's airport of Fiumicino.* Geophysical Research Letters, DOI: 10.1002/2013GL058132

Colosimo P. (1974) - *Il dissesto di Viale Tiziano in Roma: Studio di geologia ambientale applicato alla tecnologia dell'Architettura.* Geologia Tecnica, 3/1974

Corazza A., Leone F. & Mazza R. (2002) - *Il quartiere di Monteverde a Roma: sviluppo urbanistico e dissesti in un'area urbana*. Geologia dell'Ambiente - Anno **X** - 1/2002.

CPTI04 (2004) - *Catalogo parametrico dei Terremoti Italiani dal 217 a.C. al 2002.* INGV. Website *http://emidius.mi.ingv.it/cPti04/*

DBMI04 (2004) - *Database macrosismico Italiano*. INGV. Website *http://emidius.mi.ingv.it/Dbmi04*

De Angelis D'Ossat G. (1932) - *La geologia e le catacombe romane/ memoria quinta di Gioacchino de Angelis D'Ossat.* Memorie della Pontificia Accademia delle Scienze, Nuovi Lincei, S.2, **16**: 873-911-

DISS Working Group (2010). *Database of Individual Seismogenic Sources (DISS), Version 3.1.1: A compilation of potential sources for earthquakes larger than M 5.5 in Italy and surrounding areas*. http://diss.rm.ingv.it/diss/, © INGV 2010 - Istituto Nazionale di Geofisica e Vulcanologia - All rights reserved; DOI:10.6092/INGV.IT-DISS3.1.1

EUMETSAT - *Monitoring weather and climate from the space. Copyright {2014}* EUMETSAT. *http://www.eumetsat.in*

Faccena C., Funiciello R. & Marra F. (1995) - *Inquadramento geologico strutturale dell'area romana*. In *La Geologia di Roma - Il centro storico.* Memorie Descrittive della Carta Geologica D'Italia **50**: 31-47.

Frosini P. (1977) - *Il Tevere, le inondazioni di Roma e i provvedimenti presi dal governo italiano per evitarle*. Accademia Nazionale dei Lincei. Roma.

Funicello R. & Giordano G. (2008a) - Foglio 374 - Roma. Carta Geologica d'Italia alla scala 1:50.000 - Progetto CARG.

Funicello R. & Giordano G. (2008b) - *La nuova Carta geologica di Roma: Litostratigrafia ed organizzazione stratigrafica*. In: *La geologia di Roma. Dal centro storico alla periferia.* Memorie Descrittive della Carta Geologica d'Italia, **80**: 39-85.

Greenwood J.A., Landwehr J.M., Matalas N.C. & Wallis J.R. (1979) - *Probability weighted moments: definition and relation to parameters of several distribution expressable in inverse form.* Water Resources Research, **15(5)**: 1049-1054.

Giordano G. (2008) - *I vulcani di Roma: storia eruttiva e pericolosità.* In Funiciello R., Praturlon A. & Giordano G. (ed) - *La Geologia di Roma.* Memorie Descrittive della Carta Geologica d'Italia, **80**: 87-96.

Heiken G., Funiciello R., De Rita D. & Parotto M. (2006) - *I sette colli Guida geologica a una Roma mai vista*. Milano, Raffaello Cortina.

Hosking J.R.M., Wallis J.R., Wood E.F. (1984) - *Estimation of the generalized extreme value distribution by the method of probability weighted moments.*

Institute of Hydrology, Report no. 89, Wallingford, England, **27**: 251-261.

IFFI (2007) - *Inventario dei fenomeni franosi in italia realizzato dall'ISPRA e dalle Regioni e Province Autonome. http://www.isprambiente.gov.it/it/progetti/iffi-inventario-dei-fenomeni-franosi-in-italia*

INGV (2009) - *Mappa sul risentimento macrosismico del terremoto del 6 aprile 2009. http//terremoto.rm.ingv.it*

Karner D.B. & Marra F. (1998) - *Correlation of fluviodeltaic aggradational sections with glacial climate history: a revision of the classical Pleistocene stratigraphy of Rome.* Geol. Soc. Am. Bull., **110**: 748-758.

Le Gall J. (1953) - *Le Tibre fleuve de Rome dans l'Antiquitè*. Publ. de l'Institut d'Art et d'Archéologie de l'Université de Paris. Paris.

Leone F. (2014) - *L'evento alluvionale di inzio anno che ha interessato l'area romana.* Professione Geologo, **39**: 15-16.

Luciani R. (1985) - *Roma sotterranea*. Catalogo della mostra. Comune di Roma - Ass.to alla Cultura. Fratelli Palombi Editori. Roma.

Marra F. & Rosa C. (1995) - *Stratigrafia e assetto geologico dell'area romana.* In *La Geologia di Roma. Il centro storico*. Mem. Descr. Carta Geol. d'It., **50**: 49-118.

Molin D., Castenetto S., Di Loreto E., Guidoboni E., Liperi L., Narcisi B., Paciello A., Riguzzi F., Rossi A., Tertuliani A. & Trania G. (1995) - *Caratteri della sismicità*. Mem. Descr. Carta Geol. d'It., **5**: 391-403.

Jenkinson A.F. (1955) - *The frequency distribution of the annual maximum (or minimum) values of meteorological events.* Quarterly Journal of the Royal Meteorological Society, **87**: 158-171.

Karner D.B., Marra F. & Renne P.R. (2001b) - *The history of the Monti Sabatini and Alban Hills volcanoes: groundwork for assessing volcanic-tectonic hazards for Rome.* J. Volc. and Geoth. Res., **107**: 185-215.

PAI (2012) - *Piano di Assetto Idrogeologico* a cura dell'Autorità di bacino del Tevere.

PRG Roma (2007) - *Carta di pericolosità e vulnerabilità geologica del territorio comunale.* Piano Regolatore Generale del Comune di Roma a cura di Mordiagliani D.

Parotto M. (2008) - *Evoluzione paleogeografica dell'area romana: una breve sintesi.* In: *La geologia di Roma. Dal centro storico alla periferia.* Mem. Descr. Carta Geol. d'It., **80**: 25-38.

Pinna M. (1977) - *Climatologia.* UTET, Torino. XV, 442 pp.: ill.; 24 cm + 4 c. di tav.

Prestininzi A. (2000) - *La valutazione del rischio di frana: metodologie ed applicazioni al territorio della Regione Lazio.* Dipartimento di Scienze della Terra. Volume Unico, Regione Lazio con CD allegato.

Prestininzi A., Pugliese A. & Romeo R.W. (2005) - *Proposed seismic classification of Italy and related actions*. Italian Journal of Engineering Geology and Environment, 05/1. DOI:10.4408/IJEGE.2005-01.O-04.

Remedia G., Alessandroni M.G. & Mangianti F. (1998) - *Le piene eccezionali del fiume Tevere a Roma Ripetta*. Università degli Studi di L'Aquila, Dip. di Ingegneria delle Strutture, delle Acque e del Terreno (DISAT n. 3).

Sciotti M. (1986) - *Alcune osservazioni sulla situazione stratigrafica di un'area franosa a Roma.* AGI - XVI convegno Nazionale di Geotecnica, 14-16 maggio, Bologna.

Sella P., Billi A., Mazzini I., De Filippis L., Pizzino L., Sciarra A. & Quattrocchi F. (2014) - *A newly-emerged (August 2013) artificially-triggered fumarole near the Fiumicino airport, Rome, Italy.* Journal of Volcanology and Geothermal Research (2014), DOI: 10.1016/J.JVOLGEORES.2014.05.008 (in print).

Varnes D.J. (1978) - *Slope movement types and processes*. In: Schuster R.L. & Krizek R.J. (Eds.), Special Report 176 Landslides: Analysis and Control. Transportation Research Board, National Research Council, Washington D.C., 11-33.

Received April 2014 - Accepted May 2014